Metallomics

PAPER

View Article Online
View Journal | View Issue

Cite this: *Metallomics*, 2020, **12**, 218

Intestinal response to dietary manganese depletion in *Drosophila*†

Johana Vásquez-Procopio,[a] Beatriz Osorio,[a] Leticia Cortés-Martínez,[b] Fidel Hernández-Hernández,[b] Oscar Medina-Contreras,[c] Emmanuel Ríos-Castro,[d] Aram Comjean,[e] Fangge Li,[e] Yanhui Hu,[e] Stephanie Mohr,[e] Norbert Perrimon[ef] and Fanis Missirlis*[a]

Received 5th September 2019,
Accepted 26th November 2019

DOI: 10.1039/c9mt00218a

rsc.li/metallomics

Manganese is considered essential for animal growth. Manganese ions serve as cofactors to three mitochondrial enzymes: superoxide dismutase (Sod2), arginase and glutamine synthase, and to glycosyltransferases residing in the Golgi. In *Drosophila melanogaster*, manganese has also been implicated in the formation of ceramide phosphoethanolamine, the insect's sphingomyelin analogue, a structural component of cellular membranes. Manganese overload leads to neurodegeneration and toxicity in both humans and *Drosophila*. Here, we report specific absorption and accumulation of manganese during the first week of adulthood in flies, which correlates with an increase in Sod2 activity during the same period. To test the requirement of dietary manganese for this accumulation, we generated a *Drosophila* model of manganese deficiency. Due to the lack of manganese-specific chelators, we used chemically defined media to grow the flies and deplete them of the metal. Dietary manganese depletion reduced Sod2 activity. We then examined gene and protein expression changes in the intestines of manganese depleted flies. We found adaptive responses to the presumed loss of known manganese-dependent enzymatic activities: less glutamine synthase activity (amination of glutamate to glutamine) was compensated by 50% reduction in glutaminase (deamination of glutamine to glutamate); less glycosyltransferase activity, predicted to reduce protein glycosylation, was compensated by 30% reduction in lysosomal mannosidases (protein deglycosylating enzymes); less ceramide phosphoethanolamine synthase activity was compensated by 30% reduction in the *Drosophila* sphingomyeline phospodiesterase, which could catabolize ceramide phosphoethanolamine in flies. Reduced Sod2 activity, predicted to cause superoxide-dependent iron–sulphur cluster damage, resulted in cellular iron misregulation.

Significance to metallomics

Manganese is considered an essential micronutrient in animals, although clear demonstrations of manganese deficiency are scarce. We describe a manganese deficiency study in *Drosophila melanogaster*, showing that females transfer the metal to their eggs and that young adults highly and specifically absorb the metal from their diet during the first few days of their life, presumably to support manganese-dependent enzyme activities. Manganese deficient flies offer an experimental model to investigate the physiological roles of manganese. Combining metallomic, transcriptomic and proteomic analysis, we show that intestinal cells compensate for the loss of manganese-dependent biosynthetic activities by downregulating reciprocal catabolic pathways.

[a] *Departamento de Fisiología, Biofísica y Neurociencias, Centro de Investigación y de Estudios Avanzados, Av. IPN 2508, Mexico City, 07360, Mexico. E-mail: fanis@fisio.cinvestav.mx*
[b] *Departamento de Infectómica y Patogénesis Molecular, Centro de Investigación y de Estudios Avanzados, Av. IPN 2508, Mexico City, 07360, Mexico*
[c] *Laboratorio de Investigación en Inmunología y Proteómica, Hospital Infantil de México Federico Gómez, Dr Márquez 162, Mexico City, 06720, Mexico*
[d] *Unidad de Genómica, Proteómica y Metabolómica, LaNSE, Centro de Investigación y de Estudios Avanzados, Av. IPN 2508, Mexico City, 07360, Mexico*
[e] *Department of Genetics, Harvard Medical School, Boston, Massachusetts 02115, USA*
[f] *Howard Hughes Medical Institute, Boston, Massachusetts 02115, USA*

† Electronic supplementary information (ESI) available. See DOI: 10.1039/c9mt00218a

Introduction

How animals discriminate Mn is not understood

Manganese (Mn) is considered an essential micronutrient in animals, although clear demonstrations of Mn deficiency are scarce.[1,2] Three mitochondrial enzymes function using Mn ions as cofactors: superoxide dismutase (Sod2), which converts superoxide radicals to hydrogen peroxide and oxygen, glutamine synthase (GS), which adds ammonia to glutamate and arginase (Arg), which subsequently removes the ammonia as urea.[3–5] In the Golgi apparatus, Mn serves as a cofactor to galactosyltransferases.[6–8]

In *Drosophila melanogaster* and other insects, Mn ions are also required for the formation of ceramide phosphoethanolamine, a key component of cellular membranes, through the activity of ceramide phosphoethanolamine synthase (Cpes).[9,10]

Mn accumulates in mitochondria[11] and its deficiency has been shown to reduce Sod2 and Arg activities in rats.[12,13] A number of proteins involved in the correct metallation of Sod2 from mice[14] or yeast[15,16] have been identified and mitochondrial localization of the enzyme is a key requirement for successful activation.[17] Mitochondrial iron (Fe) accumulation led to displacement of the Mn for Fe in Sod2.[18–20] This observation has also been made in *Drosophila*[21] and zebrafish,[22] leading to the proposal that Sod2 participates as a switch in mitochondrial Fe metabolism: active Sod2 enables iron–sulphur cluster biosynthesis and the preservation of these cofactors in aconitase and succinate dehydrogenase; inactive Sod2 results in superoxide signalling that disrupts the tricarboxylic acid cycle and releases ferrous Fe in the matrix for heme biosynthesis.[23] Sod2 inactivation, however, is not a direct consequence of mitochondrial Fe accumulation.[24] Setting aside the question of whether Sod2 activity is regulated under normal physiology through alternative metallation, there can be no doubt that animals have in place mechanisms to discriminate between Mn and Fe to support, amongst other enzymes, mitochondrial Sod2 activity.

Physiological responses to Mn deficiency

The regulatory mechanisms that govern Mn homeostasis are not known.[2,14,25] We lack information regarding cellular sensors and signal transduction mechanisms, presumably required for regulation.[26] There is clear evidence that exposure to excess Mn results in neurodegenerative disease in humans,[27–29] rodents,[30–32] *D. melanogaster*[33–35] and *Caenorhabditis elegans*.[36–38] Accordingly, there is significant interest in discovering treatments against manganism, which can also result from genetic causes.[39–43] Hereditary human pathologies have uncovered potential transporters involved in Mn homeostasis.[44] It has been proposed that Mn is absorbed through the divalent metal transporter,[45,46] however mutants in this transporter across different animal species are deficient in Fe but not Mn.[47–51] Looking back on how we gained insights on key regulators of other metals, a useful experimental strategy has been to generate metal deficiency and monitor genes and proteins responding to correct the imbalance.[52–56] Such an approach has not yet been applied for Mn in animal studies, despite intriguing observations in the literature on the effects of its deficiency, which can lead to metabolic,[57,58] skeletal[59–61] and neurological defects.[62–64]

Chemically defined medium to control Mn availability in *Drosophila*

Experiments in *D. melanogaster* have provided valuable information with respect to insect Fe,[65,66] Cu,[67,68] Zn[68–70] and Mn[35,71] physiology. The intestine and, connected to it, the Malpighian tubules have been studied in more detail as sites of metal absorption, accumulation and excretion,[72–77] although there is little doubt that other organs also play important roles in the regulation of metal physiology[78–84] and pathophysiology.[85–87] Metal-specific chelators can be mixed into standard laboratory food to deplete a given metal's absorption by the insect: for example bathophenanthroline sulphate depletes Fe;[88] bathocuproine sulphate depletes Cu[89] and *N*,*N*,*N*′*N*′-tetrakis-(2-pyridylmethyl)-ethylenediamine depletes Zn.[75,90] Unfortunately, we lack a Mn-specific chelator that could be used for the same purpose. Thus, in this work, we developed chemically defined media to manipulate Mn concentration in *D. melanogaster*.[91,92] We aimed to determine metal concentrations in the media that would match metal content in the flies when grown in a standard yeast and molasses food source.[93] During our experiments, others published new protocols on chemically defined diets.[94–97] Here, we report findings from three different diets, achieving gradually more stringent Mn depletion in flies. We studied the adult intestine, the presumed point of entry for dietary Mn into the fly body.

Materials and methods

Supplementary material

This study generated metallomic, transcriptomic and proteomic data, which have been deposited to public databases and are also available as supplementary material to this article. Below is a summary of these datasets and other supplementary figures.

List of supplementary files

S. Fig. 1 List of RNAi lines used in this study.

S. Fig. 2 Days to appearance of first pupa and survival to adulthood of larvae raised on different chemical diets.

S. Fig. 3 Concentration of chemicals in the defined diets used here and comparison to other published protocols.

S. Fig. 4 Metal analysis by ICP-OES of the chemical diets used in this study.

S. Fig. 5 List of primers used for the qPCR experiments.

S. Fig. 6 Validation of in-gel Sod assay through RNA interference against Sod1 and Sod2.

S. Fig. 7 Diet 3 supplemented with 0.5 ppm Mn leads to Mn accumulation in five-day-old flies.

S. Fig. 8 Metallomes of flies in which RNAi against additional v-ATPase subunits was driven by *Fer2-Gal4*.

S. Table 1 Mn in diet *versus* fly bodies. Data used to generate Fig. 2 and corresponding equation.

S. Table 2 Identification of 2D-gel protein spots in Fig. 3B by MALDI/TOF/TOF.

S. Table 3 Metallome data in whole flies following ubiquitous and tissue-specific RNAi of V-ATPase subunits.

S. Table 4 Complete RNAseq data set.

S. Table 5 RNAseq RPKM data for sets of genes with altered expression; alternative presentations by spreadsheet.

S. Table 6 Complete label-free MS data sets; experiments separated in different spreadsheets and combined.

S. Table 7 Abundant intestinal proteins.

S. Table 8 Proteins changed in abundance under Mn deficiency.

S. Table 9 Differential expression of genes and proteins; a combined analysis.

Fly stocks

Isogenic lines w^+ and w^* were generated in our laboratory.[75] Oregon R-C flies from the Perrimon lab were used in the RNAseq experiment. Oregon R-C and our isogenic w^+ flies do not carry any known laboratory mutations, and their genetic backgrounds are unrelated to one another. A list of RNAi lines used to reduce the expression of V-ATPase is provided (S. Fig. 1, ESI†) along with their identifiers from the Bloomington *Drosophila* Stock Center (BDSC; Indiana, USA). Gal4 driver lines were as follows: *Da-Gal4*,[98] *Fer2LCH-Gal4*^{21B} [here referred to simply as *Fer2-Gal4*],[73] *FB-Gal4*,[98] *Uro-Gal4* (BDSC #44416) and *NP-Gal4*^{3084}.[77] Flies were maintained and used at 25 °C.

Diets

Our standard laboratory diet is based on yeast and molasses, described previously.[93] In preparing the chemically defined diets, we assumed that our standard diet provides sufficient metal content for optimal growth and reproduction of the flies, although this assumption may require revisiting in the future. We therefore adjusted metal salt quantities to match metal content in the bodies of flies grown on the chemically defined media to that of flies grown on our standard diet. Furthermore, we monitored the time for development to adulthood, initially taking the point of view that delays in development indicated a sub-optimal growth. We discovered that addition of a small quantity of yeast was required to correct this developmental delay (S. Fig. 2, ESI†). However, we later removed the addition of yeast, not only because of the undefined components it carried along, but also in view of the finding, from Suzanne Eaton's laboratory,[99–102] that yeast lipids are sensed in the larval brain and speed up normal development.[103]

The three diets used in this study were compared to other published diets (S. Fig. 3, ESI†). After defining the elemental composition using inductively coupled plasma optic emission spectrometry (ICP-OES), we discovered high sodium content in the diet (S. Fig. 4, ESI†). We searched for the source of excess sodium by checking the elemental content of individual chemicals used, and identified the source as the casein protein from BD Biosciences. We tried switching to another provider (Sigma-Aldrich C5890), but the insolubility of their product turned out to be a harder obstacle to circumvent. We therefore reduced the protein content of the diet and removed most sodium salts in diet 2. Unfortunately, when we grew the flies without the addition of Mn in either diet 1 or diet 2, we could still detect a trace amount of the metal (S. Fig. 4, ESI†) and the flies absorbed and concentrated it without problem (exceeding 0.005 mg g^{-1} dry weight of flies). We therefore also identified the source of the Mn contaminant as yeast RNA (Sigma-Aldrich R6625) and replaced the yeast RNA with uridine and inosine (diet 3, Table 1).

Table 1 Chemically defined diet with balanced metal content, which can be used for metal depletion studies

Chemical component	Provider	Diet 3
Protein and sugar		g L^{-1}
Casein	BD Biosciences 223050	21.6
Sucrose	Sigma-Aldrich S0389	19.3
Inorganic salts		
Potassium phosphate monobasic	Merck 4873	0.10
Potassium phosphate dibasic	Sigma-Aldrich P2222	0.54
Sodium bicarbonate	Sigma-Aldrich S6297	0.064
Magnesium sulfate heptahydrate	Sigma-Aldrich M5921	0.50
Calcium chloride dehydrate	Sigma-Aldrich C5670	0.15
Zinc acetate dihydrate	Sigma-Aldrich 379786	0.006
Ferric ammonium citrate	Sigma-Aldrich F5879	0.008
Manganese sulfate monohydrate	Sigma-Aldrich M7634	0.002
Copper sulfate	Sigma-Aldrich C1297	0.0005
Ammonium molybdate	Merck 321182	0.001
Vitamins		
B1. Thiamine	Sigma-Aldrich T1270	0.006
B2. Riboflavin	Sigma-Aldrich R9504	0.005
B3. Niacin	Sigma-Aldrich N4126	0.023
B5. Calcium pantothenate	Sigma-Aldrich C8731	0.019
B6. Pyridoxine hydrochloride	Sigma-Aldrich P6280	0.003
B8. Biotin	Sigma-Aldrich B4639	0.0003
B9. Folic acid	Sigma-Aldrich F8758	0.003
C. Ascorbic acid	Sigma-Aldrich A5960	0.54
Other		
Cholesterol	Sigma-Aldrich C8667	0.29
Tryptophan	Sigma-Aldrich T0254	0.24
L-Carnitine hydrochloride	Sigma-Aldrich C0283	0.010
Choline	Sigma-Aldrich C1879	0.058
Lecithin	Sigma-Aldrich P3644	0.40
Putrescine	Sigma-Aldrich P5780	0.16
Lipoic acid	Sigma-Aldrich T1395	0.052
Myo-inositol	Sigma-Aldrich I7508	0.005
Uridine	Sigma-Aldrich U3750	0.060
Inosine	Sigma-Aldrich I4125	0.065
Agar	Oxoid LP0011	16
Propionic acid	Sigma-Aldrich P5561	10 mL L^{-1}

Elemental analysis

Fresh fly food was removed from the vials and cut into small pieces. These were placed in 15 mL falcon tubes and kept at −80 °C overnight; the following day they were freeze-dried for 24 h. The dried material was pulverized using a glass rod. A mix of male and female flies of the indicated genotype, fed the indicated diet, and grown at 25 °C, were collected at 4–7 days old unless otherwise noted and kept at −80 °C, then freeze-dried for 8 h to remove water. ICP-OES was used for metal determination. 20 mg of dry sample was digested in 1 mL acid at 200 °C for 15 min in closed vessels of MARS6 microwave digestion system (CEM Corporation, Matthews, NC, USA). Samples were diluted with water to 5 mL and metal concentrations were measured against calibration curves and a digestion blank in a PerkinElmer Optima 8300 ICP-OES instrument (Shelton, CT, USA).

Open access repository of metallomics data

We built http://www.flyrnai.org/tools/metallomes2/web/, an online resource serving both as a repository for new data upload and as a portal for data access and analysis. At the query page, users can choose to access the raw data of selected measurements for metals as well as normalized data based on a selected control. The web-based application was implemented with PHP and the Symfony PHP framework. In addition, several client-side functions rely on JavaScript and AJAX, and some

tabular displays use the DataTables.js jQuery plugin. Charts were created with C3.js, a D3 java-script plotting package. Data are stored in a back-end MySQL database. Both the website and the database are hosted by the Harvard Medical School (HMS) Research Computing group.

Proteomics

Protein preparation for 2-dimensional (2D) gel electrophoresis. For each sample, the midgut was carefully dissected from 150 adult female flies of the w^+ isogenic genotype. The flies were approximately 1 week old and derived from larvae that grew on three different variants of chemical diet 1 (S. Fig. 3, ESI†), namely the control diet, the Mn-depleted diet (no Mn added) and the Fe-depleted diet (2 ppm of Fe added, required for viability, instead of 10 ppm). Tissue proteins were extracted as previously reported[104] with some modifications. The midguts were frozen in liquid nitrogen, mechanically pulverized, suspended and homogenized in 100 μL extraction buffer [50 mM Tris–HCl pH 8, 120 mM NaCl, 0.5% IGEPAL® CA-630 (Sigma-Aldrich) and supplemented with protease inhibitor cocktail (Roche Diagnostics GmbH)]. The homogenates were stirred overnight at 4 °C. The insoluble material was removed by centrifugation (2000 rpm for 7 min at 4 °C) and the supernatant was recovered. To remove lipids and salts the supernatant was selectively precipitated with 77% trichloroacetic acid and centrifuged at 15 000 × *g* for 15 min. The pellet was washed with ice-cold acetone and resuspended in 100 μL hydration buffer [7 M urea, 2 M thiourea, 4% (w/v) CHAPS hydrate (Sigma-Aldrich), 2% (w/v) immobiline pH gradient (GE Healthcare) and supplemented with protease inhibitor cocktail (at the dose recommended by Roche Diagnostics GmbH)]. Protein concentrations were measured using the 2D Quant Kit (Amersham Biosciences, USA) according to the manufacturer's recommendations.

2D-gel electrophoresis. 250 μg of protein extract was resuspended in 140 μL of hydration buffer (see above) and applied to immobiline drystrip gels, pH 3–10 NL, 10 cm (GE Healthcare, Sweden) for 18 h at room temperature.[105] Electrofocusing was performed in an Ettan IPGphor 3 Isoelectric Focusing System (GE Healthcare, USA). The strips were incubated for 10 min in equilibration buffer (6 M urea, 75 mM Tris–HCl pH 8.8, 29.3% glycerol, 2% SDS, trace bromophenol blue) containing 1% DTT and further 10 min in 2.5% iodoacetamide (Sigma-Aldrich). For SDS-polyacrylamide gel electrophoresis (PAGE), a standard vertical electrophoresis system was used with 10% polyacrylamyde gels. The assays were conducted in biological triplicate. Gels were stained with Colloidal Coomassie Blue G-250 (Bio-Safe Coomassie Stain, Bio-Rad Laboratories, USA).

Image analysis, spot excision, destaining and drying. A digital image of the gels was obtained using scanning densitometry (ChemiDoc XRS+ system, Bio-Rad) and analyzed with PDQuest 2-D Analysis Software, version 8.0 (Bio-Rad). Individually resolved spots were excised with an EXQuest Spot Cutter (Bio-Rad) and processed following Bruker's standard protocol for in gel protein digestion with minor modifications: gel particles were washed three times with 50 mM NH_4HCO_3 and acetonitrile (Sigma-Aldrich 34967) mixed in equal proportion. The proteins were then reduced with 10 mM DTT (45 min at 56 °C) and alkylated with 55 mM iodoacetamide (20 min at room temperature in the dark). Samples were washed again with 50 mM NH_4HCO_3 and acetonitrile, the supernatant was removed and the gel particles were air-dried.

Trypsin digestion, peptide extraction and MALDI-TOF/TOF. For digestion of the proteins, the gel particles were incubated with 25 ng L^{-1} Trypsin (Gold mass spectrometry, Promega) in 25 mM NH_4HCO_3 at 37 °C overnight. The supernatants were recovered and stored at −20 °C and the gel particles were incubated a second time with 50 mM NH_4HCO_3 at 37 °C overnight and the supernatants were once again stored at −20 °C. Peptides were extracted in 50 μL trifluoroacetic acid 0.1%/acetonitrile (1 : 1) for 30 min at room temperature. All supernatants were mixed and dried in a vacuum centrifuge. Peptides were resuspended in trifluoroacetic acid and analysed using a MALDI-TOF (MS/MS) Ultraflextreme mass spectrometer (Bruker, USA). LIFT fragmentation was performed. An AnchorChip target and α-cyano-4-hydroxycinnamic acid (HCCA) matrix were used, following the dried droplet protocol suggested by the manufacturer. The laser intensity was adjusted to 50% for the acquisition of parent masses and 60–70% for fragment masses, with three or four repetitions. For the analysis, spectra with 1×10^3–1×10^4 intensity peaks were considered. The identity of the protein was matched using the Mascot search engine on the fruit fly database with the following parameters: enzyme, trypsin; missed cleavages, 1; fixed modification, carbamidomethyl C; variable modification, oxidation M; parent tolerance, 0.2 Da; fragment tolerance, 0.5 Da. Positive protein identifications were those rendering a MASCOT score higher than 30.

Relative quantification by label-free mass spectrometry (MS). For each biological replicate, 40 midguts from adult female flies, 4–7 days old, of the w^+ isogenic genotype raised on diet 3 with no Mn or 5 ppm Mn. The midguts were placed in 100 μL RIPA buffer (150 mM NaCl; 1% IGEPAL®; 0.5% sodium deoxycholate; 0.1% SDS; 50 mM Tris pH 8.0) supplemented with protease inhibitor cocktail (Roche Diagnostics GmbH). The tissues were frozen and homogenized in liquid nitrogen. 300 μL RIPA buffer was added to the homogenate and stirred for 2 h at 4 °C. The homogenate was centrifuged at 13 000 rpm for 10 min. 500 μL of acetone was added to the supernatant overnight at −20 °C. The protein was precipitated by centrifugation at 15 000 rpm for 20 minutes; the pellet was resuspended in 50 μL of LAEMMLI buffer. Protein concentrations were measured using the BCA Protein Assay (Thermo Fisher Scientific) according to the manufacturer's recommendations. Next, 45 μg of a protein pool for each condition and biological replicate were subjected to 10% SDS-PAGE, allowed to advance for about 1 cm within the gel; the resulting gel fragments were enzymatically digested according to the modified protocol of Shevchenko *et al.*[106] Tryptic peptides were injected into the mass spectrometer Synapt G2-S*i* (Waters, Milford, MA) in the MS^E mode. The area under curve of the total ion chromatogram was calculated and used to normalize the samples prior to injecting into the nanoUPLC. The same amount of tryptic peptides for each condition were loaded into a Symmetry C18 Trap V/M precolumn;

180 μm × 20 mm, 100 Å pore size, 5 μm particle size. For desalting, mobile phase A, 0.1% formic acid (FA) in H_2O and mobile phase B, 0.1% FA in acetonitrile were used under the following isocratic gradient: 99.9% mobile phase A and 0.1% of mobile phase B at a flow of 5 μL min^{-1} during 3 min. Afterwards, the peptides were loaded and separated on an HSS T3 C18 Column; 75 μm × 150 mm, 100 Å pore size, 1.8 μm particle size; using an UPLC ACQUITY M-Class with the same mobile phases under the following gradient: 0 min 7% B, 121.49 min 40% B, 123.15 to 126.46 min 85% B, 129 to 130 min 7% B, at a flow of 400 nL min^{-1} and 45 °C. The spectra were acquired in a mass spectrometer with electrospray ionization and ion mobility separation Synapt G2-S*i*, using the data-independent acquisition approach through $HDMS^E$ mode (Waters, Milford, MA). At the tune page, for the ionization source, parameters were set with the following values: 2.75 kV in the sampler capilar, 30 V in the sampling cone, 30 V in the source offset, 70 °C for the source temperature, 0.5 Bar for the nano flow gas and 150 L h^{-1} for the purge gas flow. Low and high energy chromatograms were acquired in positive mode in a range of *m*/*z* 50–2000 with a scan time of 500 ms. No collision energy was applied to obtain the low energy chromatogram while for the high energy chromatograms, the precursor ions were fragmented in the transfer using a collision energy ramp from 19–55 V. The resulting *.raw files were analyzed in the DriftScope *v*2.8 software (Waters, Milford, MA) with the goal of the selective apply quasi-specific collision energies based on the drift time for each peptide detected in the mass spectrometer. A rule (*.rul) file was generated and used to apply a collision energy for every peptide detected in the $UDMS^E$ mode (instead of a linear ramp as in the $HDMS^E$ mode). With the same chromatographic and source conditions used in the $HDMS^E$ mode, tryptic peptides for each condition were injected 3 times (technical replicates) and the $UDMS^E$ mode was applied accordingly.

Data analysis. The MS proteomics data have been deposited to the ProteomeXchange Consortium *via* the PRIDE[107] partner repository with the dataset identifier PXD015543. The MS and MS/MS measurements contained into the generated *.raw files were normalized, aligned, identified,[108] compared and relatively quantified using Progenesis QI for Proteomics software *v*4.1 (Waters, Milford, MA)[109] against a *D. melanogaster* *.fasta database (downloaded from Uniprot, containing 21922 protein sequences, last modification in 26th January 2019), concatenated with its reverse.[110] The parameters used for the protein identification were: trypsin as an enzyme and one missed cleavage allowed; carbamidomethyl (C) as a fixed modification and oxidation (M), phosphoryl (S, T, Y) as variable modifications; default peptide and fragment tolerance (maximum normal distribution of 10 ppm and 20 ppm respectively) and false discovery rate ≤4%. Synapt G2-S*i* was calibrated with [Glu1]-fibrinopeptide fragments, through the precursor ion $[M + 2H]^{2+}$ = 785.84261 fragmentation of 32 eV with a result less than 1.4 ppm across all MS/MS measurements. The results generated from Progenesis software were exported to *.xlsx files in order to verify two levels of data quality control for label-free experiments (peptide and protein level) in accordance with the figures of merit described by Souza *et al.*[111] During the analysis of each experiment independently, all proteins considered differentially expressed display at least a ratio of ±1 (expressed as a base 2 logarithm); meaning that these proteins had at least ±2-absolute fold change. The ratio was calculated based on the average MS signal response of the three most intense tryptic peptides (Hi3) of each characterized protein in the Mn-depleted by control samples. For the second experiment, slightly more protein was injected into the MS for the 0 ppm Mn condition. Raw data for this condition were corrected by a factor of 0.8373, *i.e.* the calculated ratio of the total sum of intensities for each condition (S. Table 6, ESI†). Next, to directly compare between the two experiments all data from Experiment 2 were corrected by a factor of 1.452, calculated ratio of average intensity per protein (S. Table 6, ESI†).

RNAseq

RNA preparation. All flies used in this experiment were wild type of the Oregon R-C genotype. 10 females and 10 males were mated and allowed to lay eggs for five days on two variants of chemical diet 2: no Mn added or 5 ppm Mn. Parents were removed and recently-eclosed females were transferred to fresh medium for another five days. 10 midguts were dissected in PBS and homogenized in TRIzol (Invitrogen). RNA extraction and purification was performed using the Direct-zol RNAMicroPrepkit (Zymo Research) method. Two biological replicates were used for each dietary treatment group. The RNA was eluted with sterile water and each RNA solution was divided into two aliquots, one of which was freshly used to obtain an RNA Integrity Number (RIN) evaluation at the Harvard Medical School Biopolymers Facility. For samples with RIN > 6.7 and no RNA degradation, the other aliquot stored at −80 °C was submitted for sequencing.

Sequencing and analysis. The RNA libraries were prepared for sequencing using standard Illumina protocols and sequenced by Illumina NextSeq 500 instrument with a mid-output kit at the BPF Next-Gen Sequencing Core Facility at HMS. Reads were aligned to the *Drosophila* genome version dm6.24 with STAR version 2.5.2b, and counts were normalized to RPKM values with R. The raw data files as well as processed data of RPKM values have been submitted to Gene Expression Omnibus and the accession is GSE136676. Differentially expressed genes were selected based on both fold change compared to the control and adjusted *p*-value as calculated using DESeq2. High-confidence 'hits' (differentially expressed genes) were selected if 1.5 or more-fold changes were consistent between replicates and the adjusted *p*-value was less than 0.05. Genes that meet one but not both criteria were included as low-confidence hits.

Quantitative reverse transcription polymerase chain reactions. Total RNA was isolated from midguts, treated with DNase (Invitrogen), and the cDNA was prepared using oligo-dT and Superscript II (Invitrogen). The SYBR® Green PCR Mastermix and the StepOnePlus Real-Time PCR System (Applied Biosystems) were used along with primers designed using FlyPrimerBank (S. Fig. 5, ESI†).[112] The results were calculated using the $2^{-\Delta\Delta CT}$ method.[113] We selected as

a control reference primers for the gene *ZnT63C*,[114,115] which encodes a Zn transporter and whose expression was unaffected by the Mn treatment as judged by the constant and very similar CT values in all experiments.

pH determinations in the intestinal lumen

pH was assessed qualitatively in the adult midgut of flies using thymol blue (Sigma-Aldrich), as previously described.[116] The pH indicator was mixed into melted *Drosophila* diet (0.1% w/v) and allowed to cool to room temperature. Adult female flies of the appropriated genotype were allowed to feed on this food for three days. Midguts were dissected in PBS and imaged using an EZ4 HD stereomicroscope (Leica, Germany).

In-gel assay for Sod activity

Sod activity in fly extracts was assayed following native electrophoresis as previously described[117] with minor modifications. 30 adult females of indicated age were homogenized on ice-cold extraction buffer (137 mM NaCl, 20 mM Tris–HCl and Triton X-100 pH 7.5). The extract was centrifuged at 14 000 rpm for 15 min and the supernatant was transferred to a new tube. To remove lipids, the extract was centrifuged a second time at 14 000 rpm for 15 min. The supernatant was recovered and assayed for Sod activity using an in-gel activity assay after separation of the different Sod enzymes expressed in flies[118] by native protein gel electrophoresis. Gels containing electrophoresed protein samples were incubated in 2.5 mM nitroblue tetrazolium (Sigma-Aldrich) and 100 mM potassium phosphate buffer pH 7 for 20 min in the dark under gentle agitation. Gels were washed briefly in 100 mM phosphate buffer and then incubated in 28 mM *N*,*N*,*N*′,*N*′-tetramethylethylenediamine (Bio-Rad), 28 μM riboflavin (Sigma-Aldrich), 100 mM potassium phosphate (Sigma-Aldrich) for 15 min in the dark with gentle agitation. Following a brief wash in 100 mM potassium phosphate buffer, gels were exposed to white light until full colour development and photographed using an ImageQuant™ LAS 400 biomolecular imager. Due to the inherent noise from gel to gel, densitometric analysis was internally normalized; either for each sample between the single Sod2 band and the major Sod1 band (Fig. 1D) or across each gel for Sod1 and Sod2 bands (Fig. 1E). In the latter case, we normalized the intensity of the Sod bands in the samples from flies grown on 0 ppm Mn to the samples from flies grown on 2 ppm Mn, and repeated the same normalization for flies grown on 5 ppm Mn. The correspondence of each activity to the respective Sod was verified using RNA interference (S. Fig. 6, ESI†).

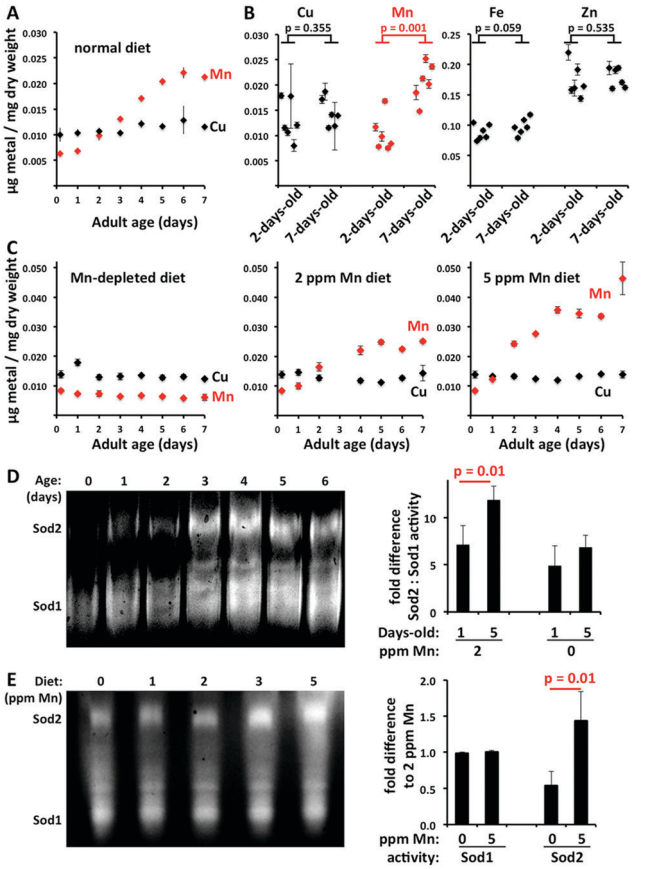

Fig. 1 The Mn concentration doubles during the first week of adult life. (A) Representative experiment showing Mn and Cu concentrations on successive days of the first week of adult life of the *D. melanogaster* w^+ strain. (B) The metallomes (Cu, Mn, Fe, Zn) were determined in six biological replicates performed at different times using 2-day-old and 7-day-old flies. The 2-way paired Students *t* test was applied for statistical analysis. (C) Freshly eclosed flies were transferred to chemically defined media with varying content of Mn added, as indicated. Mn and Cu concentrations were determined in the flies on successive days. (D) Representative in-gel assay showing Mn superoxide dismutase (Sod2) and Cu–Zn superoxide dismutase (Sod1) activities on successive days of the first week of adult life of the *D. melanogaster* w^+ strain. On the right panel, flies were shifted upon eclosure to diets with 0 or 2 ppm Mn and the quantification of the ratio between Sod2 and Sod1 activities is shown for day 1 *versus* day 5. The 2-way paired Students *t* test was applied for statistical analysis of the data from four biological replicates. The age-dependent relative increase in Sod2 activity was abrogated under Mn deprivation. (E) Representative in-gel assay for Sod activities from flies grown with indicated ppm concentrations of Mn. Quantification on the left panel was performed by using the activity determined on 2 ppm Mn as a reference point and comparing adults grown on 0 and 5 ppm Mn, respectively. The 2-way paired Students *t* test was applied for statistical analysis (four biological replicates). Whereas Sod1 activity did not change, Sod2 activity was affected by dietary Mn availability.

Results

Evidence that *D. melanogaster* discriminates Mn from Fe, Cu and Zn

We first determined the metallomes of wild-type flies in the context of our standard lab food. We noticed an abrupt change in the concentration of Mn during the first week of adult life (Fig. 1A). In these experiments, we used the isogenic strain w^+ generated through sequential back-crossing of single pairs of flies.[75] The mean value for Mn concentration in the bodies of 2-day-old young adult flies of mixed sex (reared on our laboratory's standard diet of yeast and molasses) was 0.011 ± 0.004 μg per mg dry weight (Fig. 1B). The mean value for Mn concentration in the body of 7-day-old young adult flies was 0.021 ± 0.003 μg per mg dry weight. We also confirmed that the reported results are similar

in both sexes when assayed separately and in different genetic backgrounds (data not shown). After day 6, little or no further increase in Mn was observed. Cu, Zn and Fe were determined in parallel in the same samples and did not change between 2-day-old and 7-day-old flies (Fig. 1B). Thus, we observed a doubling of Mn concentration, with no change in the other transition metals, in the course of the first few days of adulthood.

We determined in parallel the metal concentrations in the diet and the results were 0.012 ± 0.007, 0.004 ± 0.004, 0.025 ± 0.007 and 0.052 ± 0.009 μg per mg dry weight of diet, for Mn, Cu, Fe and Zn, respectively (S. Fig. 4, ESI†). High standard deviations in these measurements are attributed to variability associated with the commercial supply of molasses and yeast paste. Application of a chemically defined diet (Table 1) allowed us to regulate dietary Mn at 0.0003 mg per g dry diet weight when no Mn was added to 0.0227 ± 0.0088 mg per g dry weight when 5 ppm of Mn were added, respectively (S. Fig. 4, ESI†). We transferred freshly eclosed flies grown as larvae on standard diet to chemically defined, Mn-depleted media. This manipulation abrogated the observed increase in Mn in the flies, suggesting that the source of the accumulated Mn was dietary (Fig. 1C). In contrast, 5 ppm Mn led to a slight overloading of the metal in flies.

In our standard diet there is on average 110% more Fe and 333% more Zn in comparison to Mn, but these other elements are not preferentially absorbed. The preferential absorption of Mn in the young adult fly occurs despite Mn not being present in relative excess in the diet. To prepare the chemically defined media, we add 6 ppm Zn and 8 ppm Fe (Table 1). We asked what was the minimum concentration of Mn supplementation to observe accumulation of Mn in young adult flies; addition of 0.5 ppm Mn was readily absorbed and concentrated in the animal (S. Fig. 7, ESI†). We conclude that a presently unknown physiological mechanism operates to discriminate between Mn and the other metals.

Fly eclosure from pupal cases is associated with the formation of reactive oxygen species.[118–121] We therefore wondered whether the observed increase in total body Mn correlated with mitochondrial Sod2 activity during the same period and found evidence in support of this notion (Fig. 1D). Importantly, the increase in Sod2 activity required Mn in the diet. Furthermore, growing the flies as larvae on 5 ppm Mn resulted on a 50% increase in Sod2 activity, whereas larvae raised on 0 ppm Mn showed a 50% reduction in Sod2 activity (Fig. 1E), demonstrating that the reduction in Mn accumulation in flies correlated with reduced Sod2 activity.

Body Mn accumulation as a function of Mn concentration in the diet

In the experiments performed with the chemically defined diets, we determined Mn concentrations in the diet and in the flies derived from larvae that fed on these diets. A plot of the collected data is shown (Fig. 2). We were unable to cause lethality due to absence of Mn in the diet, despite reaching concentrations that approximated 0.1 ppb, when water content is considered. Given that there is maternal contribution of Fe during oogenesis[80] and also no observable increase in Mn concentration when adult flies are maintained on the strict Mn-depleted treatment (Fig. 1C), we suggest that the 0.002 mg Mn per g dry weight of adult fly we detect in flies raised on Mn-depleted diet (Fig. 2) was provided to the flies from deposition in the eggs from their mothers.

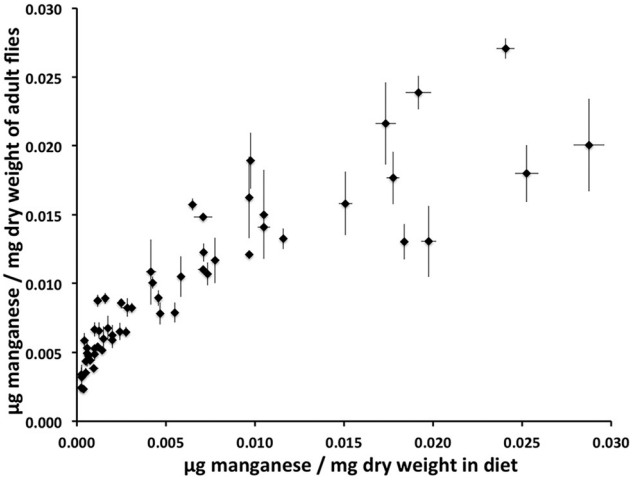

Fig. 2 Plot of dietary Mn *versus* total body Mn accumulation. Each point represents the results of experiments in which Mn was determined by ICP-OES in the diet (standard deviations tend to be smaller on the *x*-axis) and in flies, 4–7 days old, reared from embryos on the given chemical diet (a minimum of 3 independent samples were determined per point; mean and standard deviation are shown).

The distribution of data in these experiments suggested they could be fitted to a typical saturation curve using the Hill equation. When the dietary Mn concentration was less than 1 ppm, small increments in dietary Mn resulted in large increments in total body Mn concentration. In contrast, when dietary Mn concentration varied between 3 and 10 ppm, there was little change in total Mn concentration in the flies. The latter values fluctuated widely between 0.012 and 0.027 mg per g dry weight; however, these fluctuations did not correlate with dietary Mn, but are more readily explained by assuming small shifts in the mean age of flies (Fig. 1). We became aware of the changes that normally take place in Mn accumulation during the first week of life, *i.e.* the time period we collected the flies for these experiments, halfway through the experiments. Using all the available data (56 correlations in total) we generated a new plot where the lowest values approximate zero on both the *x* axis (no adjustment required) and the *y* axis, where we subtracted 0.002 mg Mn per g dry weight – that we assumed is due to maternal contribution – from each mean body Mn value (S. Table 1, ESI†). Using the Prism software, a Michaelis–Menten type function was calculated (R^2 = 0.806, 166 degrees of freedom) which we then incorporated in the following general formula:

$$y = 0.002 + \frac{0.024x}{0.008 + x}$$

where *y* is the Mn concentration given in mg per g dry weight in young adult flies and *x* is the equivalent concentration of Mn in

the diet. The equation predicts that the w^+ flies grown on an adequate supply of Mn will tend to accumulate 0.026 ± 0.001 mg metal per g body dry weight, whereas the dietary concentration at which this value is half was calculated at 0.008 ± 0.001 mg metal per diet dry weight. Converting this latter value in molarity, we suggest that the fly transporter involved in Mn uptake should show an affinity of 0.15 ± 0.02 μM for the metal.

Comparison by 2D-gel electrophoresis of the intestinal proteomes from flies fed on low Mn or Fe

Our initial experiments comparing the intestinal response of flies raised on high *versus* low Mn were performed on variants of diet 1 (S. Fig. 3 and 4, ESI†). We first demonstrated that we could specifically alter Mn concentration in flies, showing that in the group raised with no added Mn, the flies accumulated significantly lower Mn, but not Cu, Fe or Zn compared to flies on the control, Mn-supplemented, diet (Fig. 3A). As a second control group, we decided to raise flies under low Fe. The low Fe treatment has 2 ppm of this metal in the diet because when larvae were allowed to grow with no addition of Fe they were severely delayed in their growth (S. Fig. 2, ESI†) and frequently failed to initiate metamorphosis.[81] The low Fe treatment group of flies showed a moderate reduction in Fe concentration, without changes in Mn, Cu or Zn, compared to the low Mn and the control (diet 1) groups (Fig. 3A).

The midgut portion of the intestine was dissected from 4–7 day old female flies raised on the respective diets. Proteins were extracted and subjected to 2D electrophoresis. The experiment was performed three times independently. Prior to describing the comparison between the groups, we show a representative image of the intestinal proteome (Fig. 3B). Published information of the adult midgut proteome in *D. melanogaster* is limited,[122] despite extensive characterization of gene expression in the same tissue[123–125] and wide interest in its physiology.[76,126] We identified roughly 90 protein spots that were reproducibly present in the 2D-gels when 250 μg of total protein extract was used and we successfully obtained MS information for 57 of these (S. Table 2, ESI†), corresponding to 30 proteins (Table 2). These are numbered according to respective representative spots in the 2D gel shown (Fig. 3B).

The list represents a subset of the most abundant intestinal proteins, including digestive, glycolytic and stress-responsive enzymes, subunits of the F- and V-ATPase pumps, and other proteins involved in energy storage and major cytoskeletal elements (Table 2). We were mostly interested to identify intestinal proteins that responded to the lack of Mn in the diet. For this reason we compared the relative abundance of the proteomes imaged in the three independent replicates of this condition to the respective proteomes in the control diet 1 and the diet 1 supplemented with 2 ppm Fe (designated as a low-Fe condition). The comparison was performed using the PDQuest 2-D Analysis Software. Only one set of protein spots was found to be consistently upregulated in the low Mn treatment compared to the control and low Fe treatments (Fig. 3C). MS analysis revealed that the protein that was present in higher

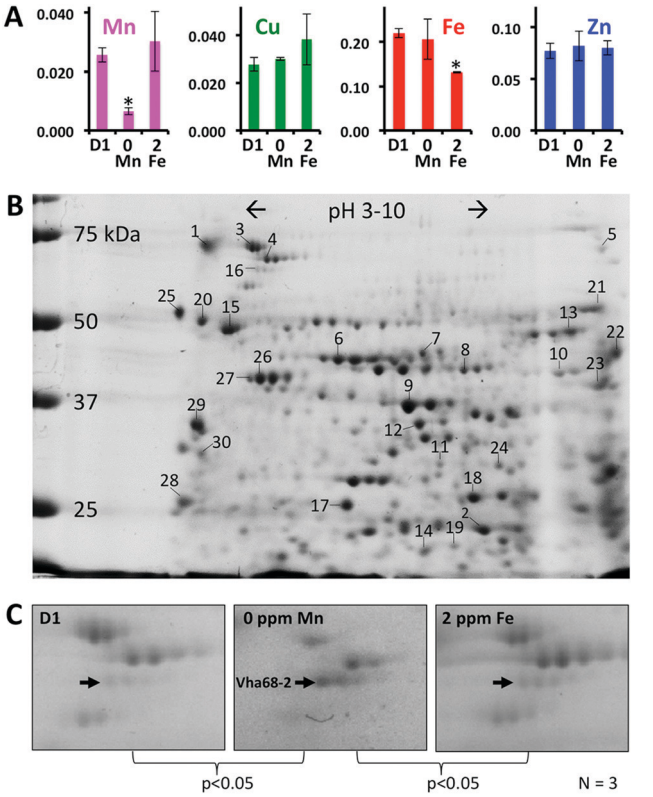

Fig. 3 Separation of the female adult intestinal proteome on 2D gels. (A) Flies of the isogenic *w** genotype were raised on diet 1 (D1), D1 without Mn (0 Mn) and D1 with only 2 (instead of 10) ppm Fe, but normal Mn concentration (2 Fe). Metal content was determined in adult flies. One-way ANOVA was used for statistical comparison of the data, generated from four independent experiments. Asterisks indicate a $p < 0.001$. (B) Protein extracts from intestines of young adult females were subjected to 2D electrophoresis, first on a pH gradient that separates proteins according to their isoelectric charge and then on a 10% acrylamide gel that separates the proteins according to their size. A representative 2D gel stained with Colloidal Coomassie Blue G-250 reveals approximately 90 protein spots, of which 57 correspond to 30 different proteins successfully characterised by MS (Table 2). (C) Three independent preparations of intestinal protein extract per condition were analysed on 2D gels using scanning densitometry and the PDQuest 2-D Analysis Software to compare the relative intensities (abundance) of each protein spot. Only one protein complex, indicated by an arrow and corresponding to the Vha68-2 protein subunit of the V-ATPase, was found to be consistently upregulated in low Mn media, compared to both control diet and low Fe diet. Close-up images of representative gels are shown.

concentration in the low Mn treated flies corresponded to Vha68-2.

The *Vha68-2* gene is highly expressed in the intestine.[116] It encodes the catalytic subunit that supports ATPase activity to the pump. Amongst the proteins identified in the gels whose expression did not change by the metal treatment, was Vha26 (Fig. 2B and Table 2) encoding another V-ATPase subunit with ubiquitous expression. The pump can be divided into two major complexes, the membrane embedded V_0 and the cytoplasmic V_1, and the pump's activity is regulated through the coupling of V_1 to V_0.[127] We further considered that other V-ATPase subunits have been implicated in Cu and Zn import in *D. melanogaster* cells[128]

Table 2 List of intestinal proteins identified by MALDI-TOF/TOF

No.	Protein	Full name and function
Digestive enzyme		
1	Mal-A1	Maltase A1 (hydrolyses dissacharides releasing glucose)
Detoxification and heat shock response		
2	Adh	Alcohol dehydrogenase
3	Hsc70-3	Heat shock protein 70 kDa cognate 3
4	Hsc70-4	Heat shock protein 70 kDa cognate 4
Lipid transport		
5	Apolpp	Apolipophorin (transports lipids, phospholipids and sterols)
6	Yp1	Yolk protein 1 (vitellogenin; lipoprotein & lipoprotein lipase)
7	Yp2	Yolk protein 2 (vitellogenin; lipoprotein & lipoprotein lipase)
8	Yp3	Yolk protein 3 (vitellogenin; lipoprotein & lipoprotein lipase)
Energy storage		
9	Argk	Arginine kinase
Glycolysis		
10	Ald1	Aldolase 1
11	Gapdh1	Glyceraldehyde-3-phosphate dehydrogenase 1
Tricarboxylic acid cycle		
12	Tpi	Triose phosphate isomerase
Proton pumps		
13	Blw	bellwether (F1F0 subunit a)
14	ATPsynD	ATP synthase, subunit D (F0 subunit D)
15	ATPsynβ	ATP synthase, subunit β (F1 subunit β)
16	Vha68-2	Vacuolar H+ ATPase 68 kDa subunit 2
17	Vha26	Vacuolar H+ ATPase 26 kDa subunit
Transport between cytoplasm and mitochondria		
18	Porin	Porin (voltage-dependent anion-selective channel)
Redox enzymes		
19	Jafrac1	Thioredoxin peroxidase 1 (2 cysteine peroxiredoxin family)
20	Pdi	Protein disulfide isomerase
21	Cat	Catalase
Transcription and protein synthesis		
22	eEF1α1	Eukaryotic translation elongation factor 1 alpha 1
23	Prp38	Pre-mRNA processing factor 38 (spliceosome component)
Signal transduction		
24	RACK1	Guanine nucleotide-binding subunit beta like protein
25	CALR	Calreticulin
Cytoskeleton		
26	Act5C	Actin 5C
27	Act79B	Actin 79B (muscle-specific)
28	Mlc2	Myosin light chain 2
29	Tm1	Tropomyosin 1 isoform 9A
30	Tm1	Tropomyosin 1 isoform 33/34

and that RNA interference against yet another subset of V-ATPase subunits rendered *D. melanogaster* cells resistant to Mn toxicity.[71] We therefore decided to ask whether the V-ATPase also plays a role in Mn homeostasis.

RNAi of V-ATPase subunit genes causes minor changes to whole-body metal accumulation

In addition to Vha68-2, two other genes encode for highly homologous catalytic A subunits that provide ATPase activity to the pump, namely Vha68-1, expressed predominantly in head and carcass, and Vha68-3, expressed predominantly in the larval fat bodies and adult testis.[129] In a typical V-ATPase pump the A subunits complex with B subunits forming a trimer of A–B dimers.[130,131] Five genes encode B subunits in *Drosophila*, but RNAi in the intestine against the *Vha100-2* subunit (amongst others) has been shown to play a key role in the acidification of the midgut[116] and was therefore selected as an extra control. We reduced expression of these subunits with RNAi and determined metal concentrations in whole fly bodies. Considering an experimental design that would minimise genetic background effects on the collected metallomes, we decided to use sibling controls and opted for the previously characterized *Fer2-Gal4* driver line,[73] which shows strong expression in the middle midgut, where also V-ATPase

expression is most pronounced[123,125] and is carried by a balancer chromosome that can act as an internal control (Fig. 4A).

Sibling flies 4–7 days old were thus separated into animals driving RNAi against the V-ATPase subunit genes and their respective controls. All lines were crossed to *Fer2-Gal4* and their progeny assayed using ICP-OES to determine their whole body metallomes raised under our standard yeast and molasses diet. The accumulation of the alkali metals sodium and potassium, the alkaline earth metals calcium and magnesium, the transition metals Mn, Fe, Cu and Zn, as well as phosphorus were quantified for each genotype several times independently (S. Table 3, ESI†). To provide easy access to the large quantity of data we generated an online, open repository at http://www.flyrnai.org/tools/metallomes2/web/.

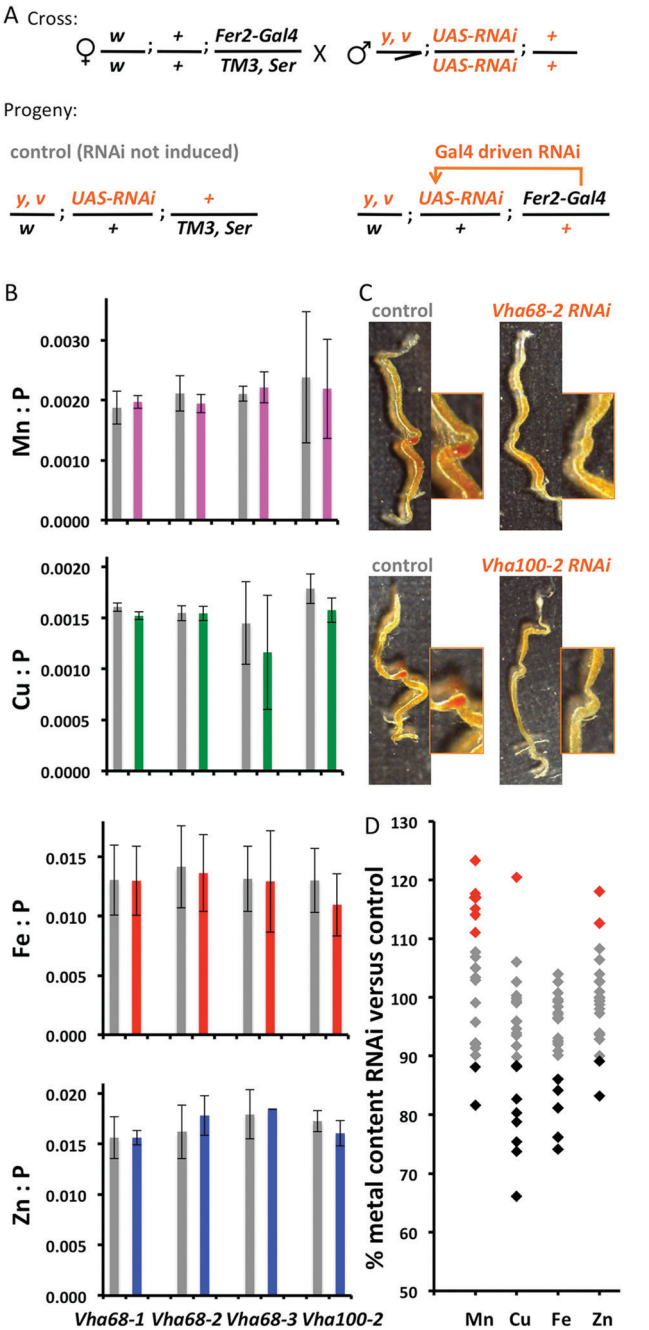

Fig. 4 Metallomes of flies in which RNAi against specific v-ATPase subunits was driven by *Fer2-Gal4*. (A) Sibling genotypes resulting from the *UAS*-Gal4 system[132] are shown. (B) Metallomes were determined by ICP-OES in control (grey bars) and experimental (coloured bars) flies. No statistically significant differences were detected by one-way ANOVA. (C) The acidic region of the middle midgut was revealed feeding flies with the pH indicator thymol blue. Note that the red colour disappears in the intestines of RNAi flies. (D) The mean % difference between RNAi-driven flies and their respective controls was plotted for the indicated metals. Each point corresponds to a different V-ATPase subunit (S. Table 3, ESI†).

We highlight a few key results related to transition metal ions. Assaying whole flies, no changes were detected in Mn, Cu, Fe or Zn following RNAi against *Vha68-1*, *Vha68-2*, *Vha68-3*, *Vha100-2* using the *Fer2-Gal4* driver (Fig. 4B). We could show that RNAi was at least partially effective in reducing V-ATPase activity, because the acidity of the middle region of the intestine was lost in the RNAi flies (Fig. 4C). Therefore, the pH of the intestinal lumen does not seem to influence metal homeostasis in this insect.

We performed a similar analysis for all the V-ATPase subunits listed in S. Fig. 1 (ESI†) and noticed that in some cases there was a tendency to change metal accumulation following RNAi compared with sibling controls (Fig. 4D). Given our relatively small number of independent replicates (between two and six per genotype, on some occasions due to semi-lethality associated with the RNAi) we did not acquire strong statistical power for our results. Nevertheless, using an arbitrary cut-off value of 10% change, we labeled red all data from genotypes where the metal concentration was higher in RNAi flies compared to controls and black for the reverse situation where RNAi appears to cause a reduction in metal concentration (Fig. 4D). Flies for which there was no change in metal concentration are shown in grey. Six of 23 of the RNAi lines showed an increase in Mn accumulation and only 2 of 23 showed a decrease. The results for Cu were different: 7 of 23 lines showed a decrease, whereas only 1 showed an increase. The overall pattern was similar between Fe and Cu, with Zn showing a more balanced response.

To take a closer look at these results, we focused on seven RNAi lines that were carried with balancer chromosomes (S. Fig. 1, ESI†), offering the opportunity to obtain two types of control sibling flies: flies carrying the RNAi transgene but lacking the driver, and flies carrying the driver but lacking the RNAi transgene (S. Fig. 8, ESI†). We considered a positive signal when the RNAi flies were different in the same direction against both sibling controls. Once again, these results did not reach statistical significance using the analysis of variance test. We nevertheless selected three lines for further scrutiny. *Vha55* and *VhaSFD* were selected on the basis that they encode unique subunits of the V_1 complex of the V-ATPase and are, accordingly, expressed ubiquitously. Intriguingly, RNAi against *Vha55* reduced the levels of Mn, Fe and Zn, but not Cu; whereas RNAi against *VhaSFD* reduced the levels of Cu, but not Mn, Fe and Zn (S. Fig. 8, ESI†). We also included *Vha16-2* in our analysis because RNAi for this subunit marginally increased Mn concentration, without affecting the other metals. *Vha16-2* is expressed

in the larval fat bodies and the adult testis and encodes for a subunit of the V_0 complex.

RNAi against *Vha55*, *VhaSFD* and *Vha16-2* was driven by four different Gal4 drivers, expressed in most cell types using an ubiquitous diver, or specifically in most cells of the midgut epithelium; in fat bodies; or in Malpighian tubules (Fig. 5). The results of these experiments can be summarised as follows: (i) ubiquitous RNAi recapitulated two of the findings with *Fer2-Gal4* driven RNAi: namely, that reduced expression of *Vha55* results in reduced accumulation of Mn, Fe and Zn, but not Cu, whereas reduced expression of *Vha16-2* results in increased Mn concentration, with little change in the other metals; (ii) RNAi of the subunits throughout the midgut or in fat bodies did not affect metal concentrations with the notable exception of Fe in the case of *Vha55*; (iii) RNAi of all three subunits in the Malpighian tubules resulted in increased Mn and decreased Zn concentrations in flies. Overall we found few effects in the global fly metallome following RNAi of V-ATPase subunits and, as shown below, no regulation of the V-ATPase subunits from dietary Mn.

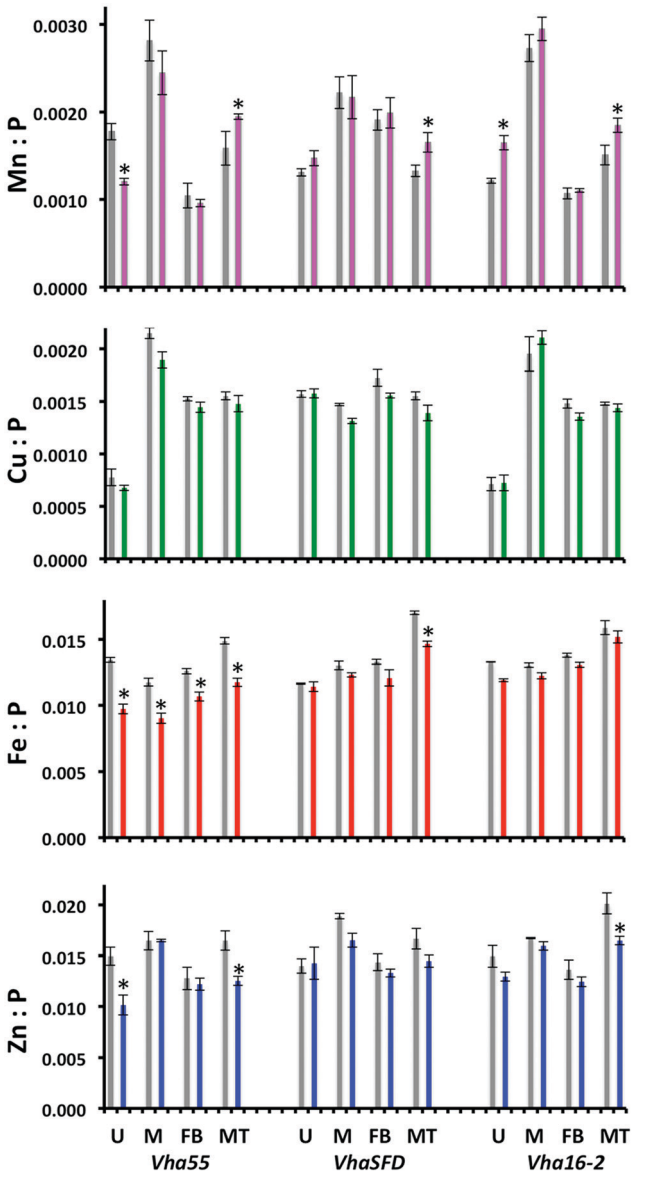

Fig. 5 Metallomes of flies in which RNAi against *Vha55*, *VhaSFD* and *Vha16-2* subunits was driven in defined organs compared to sibling controls. Metallomes were determined by ICP-OES in control (grey bars) and experimental (coloured bars) flies. Statistically significant differences at $p < 0.05$, detected by one-way ANOVA performed separately for the progeny of each driver, are marked with an asterisk. U – ubiquitous (*Da-Gal4*); M – midgut (*NP-Gal4*); FB – fat bodies (*FB-Gal4*); MT – Malpighian tubules (*Uro-Gal4*).

Intestinal gene expression changes under low dietary Mn

Diet 1 contained Mn, even when none was specifically added to the mix, because yeast is a source of metals. Our efforts to develop a treatment generating a genuine Mn deficiency led us to diet 2 (S. Fig. 3 and 4, ESI†). Besides yeast removal, other changes were informed by contemporary studies.[133] When diet 2 was used with no addition of Mn, we obtained adult populations for experiments with metal content in the diet of approximately 0.001 mg Mn per g dry weight. This condition was contrasted to diet 2 supplemented with 5 ppm Mn, which resulted in a tenfold increase of Mn in the diet and a fivefold increase of Mn content in flies that were one week old. Intestines were dissected from wild type OreR female flies grown under diet 2 with 0 or 5 ppm Mn and subjected to RNAseq analysis. The experiment was performed with two biological replicates treated separately and the full results are presented (S. Table 4, ESI†) along with a table summarizing genes that changed in expression grouped under functional categories (S. Table 5, ESI†).

A notable change in the low *versus* high Mn transcriptomes was the finding that two genes encoding for diacylglycerol acyltransferases, *Dgat2* and *CG1946*, were induced 3- and 2-fold, respectively, whereas the genes *Lip3* and *Amyrel* encoding for a lipase and an amylase, were reduced 6- and 5-fold, respectively. The changes could all be attributable to increased activity of the sugarbabe transcription factor, which regulates carbohydrate metabolism.[134,135] To validate these findings we performed qPCR for five genes and one control preparing cDNA libraries independently. We confirmed by qPCR that *Lip3*, *Amyrel* and *prt*[136] were downregulated in the Mn-depleted intestine and that *CG1946* was upregulated (Fig. 6A). In contrast, *sug* expression was variable between experiments. Below, we discuss the rest of the findings from the RNAseq experiment in a combined analysis that includes data from a second proteomic experiment.

Relative quantification of the intestinal proteome by label-free MS

Individual analysis by ICP-OES of all dietary components showed that yeast RNA contained Mn (data not shown). For this reason yeast RNA was replaced with uridine and inosine (Table 1). Making this change we were able to further reduce dietary Mn along with evidence that under this condition Sod2 activity was also affected (Fig. 1). Intestines were dissected from female w^+ isogenic flies grown with 0 or 5 ppm Mn and subjected to label-free MS analysis. The experiment was performed after

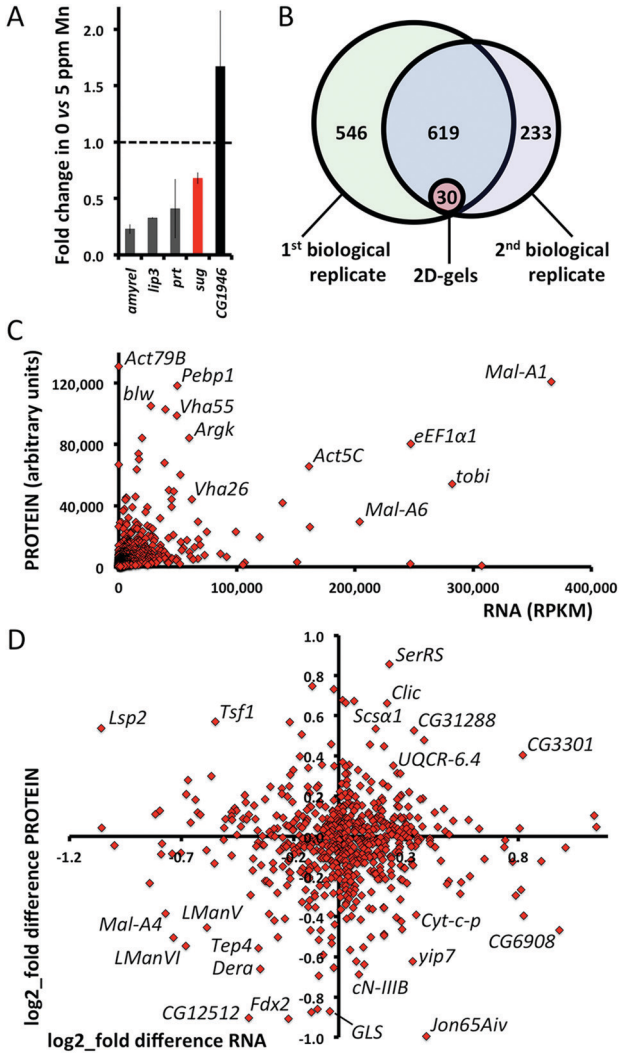

Fig. 6 Correlations between mRNA and protein. (A) qPCR results of 5 genes selected for validation of the RNAseq data. Black coloured bars indicate changes in same direction as the high-throughput experiment; the red coloured bar represents the *sug* gene, which had shown a (not statistically significant) increase in the RNAseq experiment, but was selected for further study because the sug transcription factor regulates positively *CG1946* and negatively *amyrel* and *lip3*. (B) A total of 1482 intestinal proteins were detected in this study, 649 of which were seen on both label free MS experiments. (C) Quantifications of the 649 proteins were matched to their corresponding RNAs (S. Table 9, ESI†). Only a poor overall correlation between RNA and protein abundance was found (R^2 = 0.15). Some abundant proteins are indicated. (D) Likewise, all types of correlations were seen in the directionality of expression changes for RNA and protein. Specific findings are discussed in the main text.

pooling three biological replicates per condition and repeated twice. The full results are presented (S. Table 6, ESI†) along with tables focusing on the one hundred most abundant proteins (S. Table 7, ESI†) and on the proteins that changed in abundance, grouped under functional categories, in the two experiments (S. Table 8, ESI†). Finally, we present a comparison of relative RNA and protein expression for 649 intestinal genes (S. Table 9, ESI†).

Reassuringly, all 30 proteins indicated in Table 2 were present in the quantified proteomes and six of them – Act79B, Mal-A1, eEF1α1, Argk and two subunits of the F-ATPase, ATPsynβ and Blw – were within the top 10 most abundant proteins (S. Table 7, ESI†). This set of 30 proteins changed little in abundance between the Mn depletion/supplementation groups. We did not confirm that Vha68-2 responds to Mn depletion, instead little or no change in the abundance of the V-ATPase subunits was observed (S. Table 7, ESI†). More enzymes functioning in the same functional categories represented in Table 2 were identified amongst the 100 most abundant proteins of the one week-old adult female intestine (S. Table 7, ESI†).

In total, we identified 1195 proteins in the first comparative label-free MS experiment and 882 in the second (S. Table 6, ESI†). 649 of these were common between the two experiments (Fig. 6B). We analysed the corresponding 646 genes for which we had obtained quantitative information regarding their expression at both RNA and protein level (Fig. 6C). There was limited overall correlation between proteins and their respective mRNAs in female intestines, as others have noted in similar experiments before,[137,138] although one problem with our own comparison lies in the use of different genetic backgrounds and a slightly modified diet in the two experiments. Despite this caveat, and more informative for the effect of Mn deficiency on intestinal gene and protein expression, was the comparison of the differences in expression for each of these gene/protein pairs according to treatment (Fig. 6D and S. Table 9, ESI†). We propose that upregulation of both mRNA and protein, exemplified with a number of nuclear encoded mitochondrial genes, or of genes encoding for lysosomal mannosidases in the opposite direction, provide additional confidence that the specific alterations are robust (Fig. 6D).

To facilitate the visualization and discussion of the proteomic changes observed in the Mn-depleted intestine we also generated a list of the individual proteins that showed a reproducible increase or decrease in abundance in this study (Table 3). We could readily associate a number of these with known metabolic pathways that depend on Mn: Sod2, GS, glycosyltransferases and Cpes (Arg is expressed specifically in the fat bodies, where the urea cycle takes place in insects[139]), whereas the relationship to Mn is less clear for the observed effects on serine proteases and hormone metabolising enzymes.

Abundant intestinal proteins reveal major physiological requirements of the adult intestine

Prior to discussing alterations in protein abundances upon dietary Mn depletion, we offer a brief comment on the global intestinal proteome of adult *D. melanogaster* females. The proteome of the whole intestinal tract and attached Malpighian tubules was determined previously highlighting a special role of the proteasome in these tissues.[122] Table 2 and S. Table 7 (ESI†) offer a snapshot of the protein families that are represented in abundance in the *D. melanogaster* intestine. In addition to the entire family of maltases, we detected approximately 100 proteases. Together, these secreted enzymes carry out digestive functions for carbohydrates and protein. Likewise, lipases and fatty acid binding and transport proteins are present for the absorption and

Table 3 Partial list of intestinal proteins that changed in abundance under Mn deficiency

Protein	Description	*t*-Test (p)*	5 ppm I (a.u.)**	0 ppm I (a.u.)	Ratio 0 : 5	Ref.
Loss of SOD2 activity						
Cisd2	Mitoneet|iron–sulphur clusters	0.001	3043 ± 744	2148 ± 1009	0.7	84
IRP-1A	Iron Regulatory Protein|iron sensing	0.040	1640 ± 1227	1383 ± 1012	0.8	176
Fer2LCH	Ferritin L chain|iron storage	0.000	6725 ± 1301	5526 ± 1313	0.8	177 and 178
Fer1HCH	Ferritin H chain|iron storage	0.003	9482 ± 3009	8539 ± 2843	0.9	177 and 178
Scsα1	Succinyl-CoA ligase|TCA cycle	0.000	721 ± 152	1046 ± 157	1.4	179
TFAM	Mitochondrial transcription factor A	0.005	817 ± 239	1113 ± 380	1.4	180
Tsf1	Transferrin|systemic iron trafficking	0.002	1297 ± 513	1925 ± 658	1.5	77
Clic	Chloride intracellular channel	0.007	528 ± 333	835 ± 241	1.6	181
Loss of GS activity						
GLS	Glutaminase	0.005	926 ± 395	507 ± 418	0.5	182
Gabat	Gamma-aminobutyric acid transaminase	0.017	1698 ± 1416	1228 ± 1093	0.7	183
Gs1	Glutamine synthase 1 (mitochondrial)	0.059	1256 ± 177	1044 ± 69	0.8	184
Gs2	Glutamine synthase 2 (cytoplasmic)	0.132	5370 ± 2146	4767 ± 1429	0.9	184
CG7470	Glutamate 5 kinase	0.002	16645 ± 330	19087 ± 934	1.1	185
Got1	Glutamate oxaloacetate transaminase	0.004	4779 ± 227	5096 ± 136	1.1	186
GC1***	Glutamate carrier 1	0.000	1187 ± 96	2103 ± 23	1.8	187
Gclm***	Glutamate-cysteine ligase modifier subunit	0.000	196 ± 33	531 ± 75	2.7	188
Loss of CESP activity						
αSmase***	Sphingomyelin phosphodiesterase	0.012	1450 ± 65	1041 ± 149	0.7	189
Defects in glycosylations						
LManVI	Lysosomal α-mannosidase VI	0.000	7572 ± 518	5182 ± 337	0.7	145 and 146
LManV	Lysosomal α-mannosidase V	0.000	2929 ± 517	2138 ± 410	0.7	145 and 146
Altered carbohydrate metabolism						
Pgm	Phosphoglucomutase	0.040	1043 ± 340	569 ± 102	0.5	190
Dera	Deoxyribose-phosphate aldolase	0.037	358 ± 44	227 ± 102	0.6	
Rpi	Ribose-5-phosphate isomerase	0.011	613 ± 57	504 ± 106	0.8	191
Pgi	Glucose-6-phosphate isomerase	0.028	2518 ± 302	2902 ± 514	1.2	192
Reduced serine proteases						
SP151	Serine protease	0.001	1171 ± 206	645 ± 144	0.6	193
CG4734	Serine protease	0.001	1896 ± 202	1173 ± 113	0.6	193
Altered hormonal responses						
Jheh3	Juvenile hormone epoxide hydrolase 3	0.000	1095 ± 511	782 ± 455	0.7	194
CG7953	Haemolymph juvenile hormone binding	0.003	1148 ± 550	810 ± 449	0.7	
CG3301	17-β-Estradiol 17-dehydrogenase	0.000	4309 ± 443	5703 ± 676	1.3	
CG31288	Ecdysteroid kinase like	0.020	1981 ± 228	2855 ± 443	1.4	

* The p value reported is from a paired t-test using the six technical replicates. The paired test was selected due to the differences in relative expression levels between the two biological replicates, which explain the large standard deviations in the data.** The average signal intensity (I) from the six determinations is shown in arbitrary units (a.u.) for each condition. Signal intensity was determined using the 3 most intense tryptic peptide MS signals of each protein as described in Materials and methods.*** The p value is from an unpaired t-test on triplicate technical replicates as these proteins were only detected on one of two biological replicates.

mobilisation of dietary fat. Alcohol and aldehyde dehydrogenases and numerous P450 cytochrome oxidases are present for detoxification reactions. Likewise, glutathione *S* transferases and other thiol and antioxidant defense enzymes and heat shock proteins were found. Cytoskeletal proteins of both the muscle-specific type and of enterocytes and enteroendocrine cells were abundant. Arginine kinase, an enzyme that stores ATP by conjugating it reversibly to arginine,[140,141] was highly expressed, as were both major types of proton-pumps: the F-ATPase and V-ATPase complexes. The latter has an insect-specific function in regulating intestinal pH[116] whereas the former supports oxidative phosphorylation.[142] Enzymes of the glycolytic pathway, the tricarboxylic acid cycle and the mitochondrial oxidative phosphorylation complexes were also present. Along with the protein translation and degradation machineries, the proteins noted above constitute the bulk of intestinal proteins. We conclude that the intestine generates ATP through oxygen-based respiration for transport purposes and also for generating and secreting digestive enzymes. In this way, it serves its important function of nutrient absorption.[76]

Mn deficiency alters intestinal physiology

We report dietary Mn at approximately 0.1 ppb, which reduces Sod2 activity by approximately 50% as judged by an in-gel assay (Fig. 1). Sod2 converts superoxide and protons to hydrogen peroxide and oxygen. Increased mitochondrial superoxide will disrupt iron–sulphur clusters in aconitase and succinate dehydrogenase[118,143] resulting in a block of the tricarboxylic

acid cycle and disrupted Fe homeostasis leading to cytosolic Fe deficiency.[23] We observe the hallmarks of this response in the reduction of both ferritin subunits and of the cytosolic Fe sensor IRP-1A and its repair protein Cisd-2 (Table 3);[84,144] while the increase in Tsf1 is likely the fat body's response sensing a drop in systemic Fe, secreting Tsf1, which then binds to the basolateral side of the enterocytes.[77] Furthermore, we find increases in two enzymes that mediate the flux of the tricarboxylic acid cycle between aconitase and succinate dehydrogenase, namely Scsα1 (Table 3) and isocitrate dehydrogenase (S. Table 8, ESI†).

Under these Mn-restrictive conditions we hypothesize, based on the Mn-dependence of GS activity,[5] a decrease in activity of both GS enzymes, despite their protein backbones being present (Table 3). Cells depend exclusively on GS to convert glutamate to glutamine, but they can also perform the reverse reaction using glutaminase (GLS). Furthermore, an important downstream metabolite of glutamine is GABA. Two enzymes that were found reduced in Mn deficiency are responsible for the catabolism of glutamine and GABA, respectively, providing a straightforward adaptation to their reduced biosynthesis (Table 3). Glutamate on the other hand appears to be removed by being converted to glutathione (increase in Gclm), by being trafficked to the mitochondria (increase in GC1) and by being metabolised (small increases in the glutamate 5 kinase homologue CG7470 and Got1).

Although there is only empirical evidence that Mn is required for Cpes activity and no mechanistic insight into the way it acts in the production of ceramide phosphoethanolamine,[9] the sphingomyelin phosphodiesterase that catalyses the same reaction in the opposite direction was also seen diminished by Mn deficiency, preserving in this way the membrane sphingolipid (Table 3). The reduction of αSmase (detected in one of the two experiments) provides support to the proposed physiologic requirement of Mn for ceramide phosphoethanolamine synthesis.[10] A more robust finding was the reduction in two class-II α-mannosidases (LManV & LManVI),[145] which were found diminished both at the RNA and protein levels (Fig. 6D). These enzymes are involved in the catabolism of glycoproteins and their reduction makes sense in light of the Mn requirement for the catalytic activity of glycosyltransferases.[6–8] Furthermore, a Mn-dependence has been suggested for the metallophosphoesterase (MPPE) acting directly on different class II α-mannosidase to regulate its activity.[146] Hence, the observed decrease in LManV and LManVI could also be the result of misregulated phosphorylation.

Finally, we noted changes in enzymes involved in carbohydrate and hormonal metabolism and a reduction in the presence of serine proteases (Table 3 and S. Table 8, ESI†). That Mn deficiency alters carbohydrate metabolism was also evident in the RNAseq experiment (S. Table 5, ESI†) and has been observed before in the Mn deficient rat.[57,58] The genes encoding for serine proteases were consistently upregulated (S. Table 5, ESI†), whereas the proteins were found diminished (S. Table 8, ESI†). Genes and proteins involved in the metabolism of ecdysone and juvenile hormone were widely misregulated in Mn deficiency. The physiological function of these genes is unknown, although likely connected to the broader changes that occur during the first week of adulthood.

Discussion

Metal transport selectivity

Specific Mn transport is not understood in insects. There is a view that Malvolio, the insect's DMT1 homologue,[147,148] transports Mn, based on the finding that its behavioural phenotype can be rescued by dietary Mn.[45] Our own efforts to reproduce these experiments have been unsuccessful on more than one occasion (in our hands the *Malvolio*^{97f} mutant shows sugar preference), but Ben-Shahar and colleagues have built on the earlier work.[149,150] Although there is no doubt that DMT1 can transport Mn *in vitro*,[151,152] no alteration was observed in Mn content in the *Malvolio* mutant,[47,153] perhaps because DMT1 may function as a low-affinity transporter in the micromolar range.[154] Our calculation suggests the existence of a high-affinity transport system for Mn in *D. melanogaster* (Fig. 2) with an apparent Km of 0.15 ± 0.02 μM. We note an independent report that cadmium and Mn may share a transport system in animal cells, with an apparent inhibitory K_i of 0.14 μM.[155,156]

We also note that three other mammalian transporters recently implicated in cellular Mn import, Zip8[14,157] and Zip14[43,158,159] and export, ZnT10[39, 40, 160–163] do not have orthologues in *D. melanogaster*.[115] Our results with the present Mn deficiency model have not led us to the identification of a candidate transporter, but we hope to perform proteomics analysis on membrane fractions to enrich for the transport systems of the enterocyte plasma membrane and also test more dynamic feeding regimes in search of a situation where the transport system is upregulated. A further potential reason for failing to detect the upregulation of the high-affinity Mn transport system in this study is that the treatments were compared at a time period where we discover an endogenous upregulation of Mn transport (Fig. 1).

Is there a physiological reason for the observed increase in Mn concentration during the first few days of adult life?

The doubling of Mn content during the first days following the emergence of adult *D. melanogaster* flies from their pupa cases calls for explanation. Although we show that one potential reason for such an increase may be an increased requirement of Sod2 to support aerobic metabolism (Fig. 1D and E)[118,120,121] further physiological changes may depend on the specific accumulation of Mn. Documented changes that take place during this period are the hardening and waterproofing of the insect's cuticle with underlying changes in lipid homeostasis;[164] the removal of the remnant larval fat body cells, which are dispersed in the hemolymph of recently emerged flies and are removed following hormonal signals;[165,166] and changes in brain circuitry,[167,168] photoreception[169] and related behavioural and sexual maturation events.[170–172] Our observations here and those of many other groups highlight a need to carefully control

for age-related changes during the first week of adult life; indeed during our early work we had been puzzled by the larger variability of our Mn measurements compared to Fe, Cu and Zn,[93,173] which we can now attribute to physiological changes in Mn concentration missed in the standard protocol of collecting two to seven-day-old flies used over the years. There is also much more to be learned about this understudied (in its own right) period of the life cycle of *Drosophila*. However, in concluding this report, we also wish to stress that perhaps the most striking aspect of our finding is the insect's ability to concentrate Mn specifically over Fe, Cu and Zn. The objective to identify the mechanism behind such specificity remains open to the field.

V-ATPase function in metal homeostasis

A number of different V-ATPase complexes are formed in different cell types – and possibly in different subcellular locations – of *D. melanogaster*, evidenced by multiple homologous genes encoding for some of its structural subunits and similar combinatorial gene expression patterns reported by FlyAtlas in the digestive system, the larval fat bodies and adult testis, the head and carcass.[174,175] There are also 5 genes, all encoding for subunits of the V_1 complex, whose products are unique and presumably required for all functional V-ATPase pumps (S. Fig. 1, ESI†). RNAi of some of V-ATPase subunits was protective in the context of *Drosophila* cell culture subjected to Mn overload toxicity,[71] although the mechanism involved remains to be described. RNAi of two of these genes, *Vha55* and *VhaSFD*, and of *Vha16-2* in the Malpighian tubules resulted in flies that accumulated more Mn compared to their sibling controls (Fig. 5). The same genotypes that showed an increase in total body Mn also showed a decrease in total body Zn, suggesting that the V-ATPase may be involved in opposing ways in the storage and excretion of these two metals. As our focus here has been the intestine, we did not pursue further these observations, but we note that the Malpighian tubules likely serve Mn storage and excretion functions[72] in a similar way to Zn.[75] In contrast, we were unable to discern any clear function for the V-ATPase in the intestinal absorption of Mn. Although some evidence points to a role of the V-ATPase in the absorption of Fe and Cu (Fig. 4D), we were surprised to also obtain evidence that despite neutralizing intestinal pH, metal homeostasis was seen unaffected (Fig. 4B and C). Finally, our initial observation that reducing Mn content in diet 1 – which is substantially different to diets 2 & 3 (S. Fig. 3 and 4, ESI†) – increased the abundance of the intestinal Vha68-2 subunit (Fig. 3C) was not confirmed in follow-up experiments (S. Table 7, ESI†).

Conclusions

We describe a Mn deficiency study in *D. melanogaster*, which uncovered the existence of a maternal contribution of the metal during the insect's life cycle and a specific dietary requirement during the first days of adulthood to support Sod2 and other Mn-dependent activities. As expected from the loss of Sod2 activity in the Mn-depleted intestine, Fe metabolism is affected as a result. Intestinal cells compensated the loss of GS, glycosyltransferase and Cpes activities by downregulating the reverse reaction enzymes glutaminase, lysosomal mannosidase and sphingomyelin phosphodiesterase, respectively. Serine proteases were also downregulated for reasons that remain unclear. Mn deficient flies offer an experimental model to investigate the physiological roles of Mn and help identify how Mn is sensed and trafficked in insects.

Conflicts of interest

There are no conflicts to declare.

Acknowledgements

CONACYT supported JV-P with PhD fellowship #426510, a travel fund and funded the initial stages of this work through a young investigator basic sciences grant #179835 to FM. The MARS6 microwave digestion system and the PerkinElmer OptimaTM 8300 ICP-OES instrument were acquired with the CONACYT infrastructure grant #268296. We also acknowledge funding for scientific research and technological development from Cinvestav and Mexico's Ministry of Education (project #61). We thank the BPF Next-Gen Sequencing Core Facility at Harvard Medical School and the Genomics, Proteomics and Metabolomics unit of the Central Laboratories of Cinvestav for their expertise and instrument availability that supported this work. We also thank Pedro Saavedra at Harvard Medical School for sharing protocols expertise, Dulce María del Carmen Delgadillo Álvarez and Gustavo Félix Toyos Sánchez at Cinvestav's Central Laboratories for their assistance in sample preparation for proteomic analysis. We are also grateful to three anonymous reviewers whose comments and criticisms helped improve this paper.

Notes and references

1 J. W. Finley and C. D. Davis, Manganese deficiency and toxicity: are high or low dietary amounts of manganese cause for concern?, *BioFactors*, 1999, **10**, 15–24.
2 K. J. Horning, S. W. Caito, K. G. Tipps, A. B. Bowman and M. Aschner, Manganese Is Essential for Neuronal Health, *Annu. Rev. Nutr.*, 2015, **35**, 71–108.
3 B. B. Keele Jr., J. M. McCord and I. Fridovich, Superoxide dismutase from escherichia coli B. A new manganese-containing enzyme, *J. Biol. Chem.*, 1970, **245**, 6176–6181.
4 H. Hirsch-Kolb, H. J. Kolb and D. M. Greenberg, Nuclear magnetic resonance studies of manganese binding of rat liver arginase, *J. Biol. Chem.*, 1971, **246**, 395–401.
5 W. W. Krajewski, R. Collins, L. Holmberg-Schiavone, T. A. Jones, T. Karlberg and S. L. Mowbray, Crystal structures of mammalian glutamine synthetases illustrate substrate-induced conformational changes and provide

opportunities for drug and herbicide design, *J. Mol. Biol.*, 2008, **375**, 217–228.

6 J. F. Morrison and K. E. Ebner, Studies on galactosyltransferase. Kinetic investigations with N-acetylglucosamine as the galactosyl group acceptor, *J. Biol. Chem.*, 1971, **246**, 3977–3984.

7 B. Ramakrishnan and P. K. Qasba, Comparison of the closed conformation of the beta 1,4-galactosyltransferase-1 (beta 4Gal-T1) in the presence and absence of alpha-lactalbumin (LA), *J. Biomol. Struct. Dyn.*, 2003, **21**, 1–8.

8 V. Sladek and I. Tvaroska, First-Principles Interaction Analysis Assessment of the Manganese Cation in the Catalytic Activity of Glycosyltransferases, *J. Phys. Chem. B*, 2017, **121**, 6148–6162.

9 A. M. Vacaru, J. van den Dikkenberg, P. Ternes and J. C. Holthuis, Ceramide phosphoethanolamine biosynthesis in Drosophila is mediated by a unique ethanolamine phosphotransferase in the Golgi lumen, *J. Biol. Chem.*, 2013, **288**, 11520–11530.

10 A. Panevska, M. Skocaj, I. Krizaj, P. Macek and K. Sepcic, Ceramide phosphoethanolamine, an enigmatic cellular membrane sphingolipid, *Biochimica et biophysica acta, Biomembranes*, 2019, **1861**, 1284–1292.

11 L. S. Maynard and G. C. Cotzias, The partition of manganese among organs and intracellular organelles of the rat, *J. Biol. Chem.*, 1955, **214**, 489–495.

12 S. Zidenberg-Cherr, C. L. Keen, B. Lonnerdal and L. S. Hurley, Superoxide dismutase activity and lipid peroxidation in the rat: developmental correlations affected by manganese deficiency, *J. Nutr.*, 1983, **113**, 2498–2504.

13 A. A. Brock, S. A. Chapman, E. A. Ulman and G. Wu, Dietary manganese deficiency decreases rat hepatic arginase activity, *J. Nutr.*, 1994, **124**, 340–344.

14 S. J. V. Gordon, D. E. Fenker, K. E. Vest and T. Padilla-Benavides, Manganese influx and expression of ZIP8 is essential in primary myoblasts and contributes to activation of SOD2, *Metallomics*, 2019, **11**, 1140–1153.

15 E. E. Luk and V. C. Culotta, Manganese superoxide dismutase in Saccharomyces cerevisiae acquires its metal co-factor through a pathway involving the Nramp metal transporter, Smf2p, *J. Biol. Chem.*, 2001, **276**, 47556–47562.

16 E. Luk, M. Carroll, M. Baker and V. C. Culotta, Manganese activation of superoxide dismutase 2 in Saccharomyces cerevisiae requires MTM1, a member of the mitochondrial carrier family, *Proc. Natl. Acad. Sci. U. S. A.*, 2003, **100**, 10353–10357.

17 E. Luk, M. Yang, L. T. Jensen, Y. Bourbonnais and V. C. Culotta, Manganese activation of superoxide dismutase 2 in the mitochondria of Saccharomyces cerevisiae, *J. Biol. Chem.*, 2005, **280**, 22715–22720.

18 M. Yang, P. A. Cobine, S. Molik, A. Naranuntarat, R. Lill, D. R. Winge and V. C. Culotta, The effects of mitochondrial iron homeostasis on cofactor specificity of superoxide dismutase 2, *EMBO J.*, 2006, **25**, 1775–1783.

19 V. Irazusta, E. Cabiscol, G. Reverter-Branchat, J. Ros and J. Tamarit, Manganese is the link between frataxin and iron-sulfur deficiency in the yeast model of Friedreich ataxia, *J. Biol. Chem.*, 2006, **281**, 12227–12232.

20 A. Naranuntarat, L. T. Jensen, S. Pazicni, J. E. Penner-Hahn and V. C. Culotta, The interaction of mitochondrial iron with manganese superoxide dismutase, *J. Biol. Chem.*, 2009, **284**, 22633–22640.

21 J. R. Slabbaert, S. Kuenen, J. Swerts, I. Maes, V. Uytterhoeven, J. Kasprowicz, A. C. Fernandes, R. Blust and P. Verstreken, Shawn, the Drosophila Homolog of SLC25A39/40, Is a Mitochondrial Carrier That Promotes Neuronal Survival, *J. Neurosci.*, 2016, **36**, 1914–1929.

22 R. Nilsson, I. J. Schultz, E. L. Pierce, K. A. Soltis, A. Naranuntarat, D. M. Ward, J. M. Baughman, P. N. Paradkar, P. D. Kingsley, V. C. Culotta, J. Kaplan, J. Palis, B. H. Paw and V. K. Mootha, Discovery of genes essential for heme biosynthesis through large-scale gene expression analysis, *Cell Metab.*, 2009, **10**, 119–130.

23 Z. Marelja, S. Leimkuhler and F. Missirlis, Iron Sulfur and Molybdenum Cofactor Enzymes Regulate the Drosophila Life Cycle by Controlling Cell Metabolism, *Front. Physiol.*, 2018, **9**, 50.

24 J. Park, S. P. McCormick, M. Chakrabarti and P. A. Lindahl, Insights into the iron-ome and manganese-ome of Deltamtm1 Saccharomyces cerevisiae mitochondria, *Metallomics*, 2013, **5**, 656–672.

25 A. C. Pfalzer and A. B. Bowman, Relationships Between Essential Manganese Biology and Manganese Toxicity in Neurological Disease, *Curr. Environ. Health Rep.*, 2017, **4**, 223–228.

26 G. C. Cotzias and P. S. Papavasiliou, Primordial Homeostasis in a Mammal as Shown by the Control of Manganese, *Nature*, 1964, **201**, 828–829.

27 I. Mena, O. Marin, S. Fuenzalida and G. C. Cotzias, Chronic manganese poisoning. Clinical picture and manganese turnover, *Neurology*, 1967, **17**, 128–136.

28 R. Lucchini, D. Placidi, G. Cagna, C. Fedrighi, M. Oppini, M. Peli and S. Zoni, Manganese and Developmental Neurotoxicity, *Adv. Neurobiol.*, 2017, **18**, 13–34.

29 S. Rivera-Mancia, C. Rios and S. Montes, Manganese accumulation in the CNS and associated pathologies, *Biometals*, 2011, **24**, 811–825.

30 A. Pentschew, Contribution of experimental manganese encephalopathy to neurology and neuropathology, *Rev. Neuro-Psiquiatr.*, 1964, **27**, 405–413.

31 S. V. Chandra and G. S. Shukla, Manganese encephalopathy in growing rats, *Environ. Res.*, 1978, **15**, 28–37.

32 G. Gianutsos and M. T. Murray, Alterations in brain dopamine and GABA following inorganic or organic manganese administration, *Neurotoxicology*, 1982, **3**, 75–81.

33 L. Bonilla-Ramirez, M. Jimenez-Del-Rio and C. Velez-Pardo, Acute and chronic metal exposure impairs locomotion activity in Drosophila melanogaster: a model to study Parkinsonism, *Biometals*, 2011, **24**, 1045–1057.

34 E. Bonilla, R. Contreras, S. Medina-Leendertz, M. Mora, V. Villalobos and Y. Bravo, Minocycline increases the life span and motor activity and decreases lipid peroxidation

in manganese treated Drosophila melanogaster, *Toxicology*, 2012, **294**, 50–53.

35 Y. Ben-Shahar, The Impact of Environmental Mn Exposure on Insect Biology, *Front. Genet.*, 2018, **9**, 70.

36 R. Settivari, J. Levora and R. Nass, The divalent metal transporter homologues SMF-1/2 mediate dopamine neuron sensitivity in caenorhabditis elegans models of manganism and parkinson disease, *J. Biol. Chem.*, 2009, **284**, 35758–35768.

37 A. Benedetto, C. Au, D. S. Avila, D. Milatovic and M. Aschner, Extracellular dopamine potentiates mn-induced oxidative stress, lifespan reduction, and dopaminergic neurodegeneration in a BLI-3-dependent manner in Caenorhabditis elegans, *PLoS Genet.*, 2010, **6**, e1001084.

38 S. Angeli, T. Barhydt, R. Jacobs, D. W. Killilea, G. J. Lithgow and J. K. Andersen, Manganese disturbs metal and protein homeostasis in Caenorhabditis elegans, *Metallomics*, 2014, **6**, 1816–1823.

39 M. Quadri, A. Federico, T. Zhao, G. J. Breedveld, C. Battisti, C. Delnooz, L. A. Severijnen, L. Di Toro Mammarella, A. Mignarri, L. Monti, A. Sanna, P. Lu, F. Punzo, G. Cossu, R. Willemsen, F. Rasi, B. A. Oostra, B. P. van de Warrenburg and V. Bonifati, Mutations in SLC30A10 cause parkinsonism and dystonia with hypermanganesemia, polycythemia, and chronic liver disease, *Am. J. Hum. Genet.*, 2012, **90**, 467–477.

40 K. Tuschl, P. T. Clayton, S. M. Gospe Jr., S. Gulab, S. Ibrahim, P. Singhi, R. Aulakh, R. T. Ribeiro, O. G. Barsottini, M. S. Zaki, M. L. Del Rosario, S. Dyack, V. Price, A. Rideout, K. Gordon, R. A. Wevers, W. K. Chong and P. B. Mills, Syndrome of hepatic cirrhosis, dystonia, polycythemia, and hypermanganesemia caused by mutations in SLC30A10, a manganese transporter in man, *Am. J. Hum. Genet.*, 2012, **90**, 457–466.

41 J. H. Park, M. Hogrebe, M. Gruneberg, I. DuChesne, A. L. von der Heiden, J. Reunert, K. P. Schlingmann, K. M. Boycott, C. L. Beaulieu, A. A. Mhanni, A. M. Innes, K. Hortnagel, S. Biskup, E. M. Gleixner, G. Kurlemann, B. Fiedler, H. Omran, F. Rutsch, Y. Wada, K. Tsiakas, R. Santer, D. W. Nebert, S. Rust and T. Marquardt, SLC39A8 Deficiency: A Disorder of Manganese Transport and Glycosylation, *Am. J. Hum. Genet.*, 2015, **97**, 894–903.

42 K. Tuschl, E. Meyer, L. E. Valdivia, N. Zhao, C. Dadswell, A. Abdul-Sada, C. Y. Hung, M. A. Simpson, W. K. Chong, T. S. Jacques, R. L. Woltjer, S. Eaton, A. Gregory, L. Sanford, E. Kara, H. Houlden, S. M. Cuno, H. Prokisch, L. Valletta, V. Tiranti, R. Younis, E. R. Maher, J. Spencer, A. Straatman-Iwanowska, P. Gissen, L. A. Selim, G. Pintos-Morell, W. Coroleu-Lletget, S. S. Mohammad, S. Yoganathan, R. C. Dale, M. Thomas, J. Rihel, O. A. Bodamer, C. A. Enns, S. J. Hayflick, P. T. Clayton, P. B. Mills, M. A. Kurian and S. W. Wilson, Mutations in SLC39A14 disrupt manganese homeostasis and cause childhood-onset parkinsonism-dystonia, *Nat. Commun.*, 2016, **7**, 11601.

43 S. Jenkitkasemwong, A. Akinyode, E. Paulus, R. Weiskirchen, S. Hojyo, T. Fukada, G. Giraldo, J. Schrier, A. Garcia, C. Janus, B. Giasson and M. D. Knutson, SLC39A14 deficiency alters manganese homeostasis and excretion resulting in brain manganese accumulation and motor deficits in mice, *Proc. Natl. Acad. Sci. U. S. A.*, 2018, **115**, E1769–E1778.

44 S. Anagianni and K. Tuschl, Genetic Disorders of Manganese Metabolism, *Curr. Neurol. Neurosci. Rep.*, 2019, **19**, 33.

45 S. Orgad, H. Nelson, D. Segal and N. Nelson, Metal ions suppress the abnormal taste behavior of the Drosophila mutant malvolio, *J. Exp. Biol.*, 1998, **201**, 115–120.

46 V. A. Fitsanakis, N. Zhang, S. Garcia and M. Aschner, Manganese (Mn) and iron (Fe): interdependency of transport and regulation, *Neurotoxic. Res.*, 2010, **18**, 124–131.

47 L. Bettedi, M. F. Aslam, J. Szular, K. Mandilaras and F. Missirlis, Iron depletion in the intestines of Malvolio mutant flies does not occur in the absence of a multicopper oxidase, *J. Exp. Biol.*, 2011, **214**, 971–978.

48 A. Shawki, S. R. Anthony, Y. Nose, M. A. Engevik, E. J. Niespodzany, T. Barrientos, H. Ohrvik, R. T. Worrell, D. J. Thiele and B. Mackenzie, Intestinal DMT1 is critical for iron absorption in the mouse but is not required for the absorption of copper or manganese, *Am. J. Physiol.: Gastrointest. Liver Physiol.*, 2015, **309**, G635–647.

49 M. D. Fleming, M. A. Romano, M. A. Su, L. M. Garrick, M. D. Garrick and N. C. Andrews, Nramp2 is mutated in the anemic Belgrade (b) rat: evidence of a role for Nramp2 in endosomal iron transport, *Proc. Natl. Acad. Sci. U. S. A.*, 1998, **95**, 1148–1153.

50 M. D. Fleming, C. C. Trenor 3rd, M. A. Su, D. Foernzler, D. R. Beier, W. F. Dietrich and N. C. Andrews, Microcytic anaemia mice have a mutation in Nramp2, a candidate iron transporter gene, *Nat. Genet.*, 1997, **16**, 383–386.

51 A. Donovan, A. Brownlie, M. O. Dorschner, Y. Zhou, S. J. Pratt, B. H. Paw, R. B. Phillips, C. Thisse, B. Thisse and L. I. Zon, The zebrafish mutant gene chardonnay (cdy) encodes divalent metal transporter 1 (DMT1), *Blood*, 2002, **100**, 4655–4659.

52 T. A. Rouault, M. W. Hentze, S. W. Caughman, J. B. Harford and R. D. Klausner, Binding of a cytosolic protein to the iron-responsive element of human ferritin messenger RNA, *Science*, 1988, **241**, 1207–1210.

53 R. D. Palmiter and S. D. Findley, Cloning and functional characterization of a mammalian zinc transporter that confers resistance to zinc, *EMBO J.*, 1995, **14**, 639–649.

54 N. Grotz, T. Fox, E. Connolly, W. Park, M. L. Guerinot and D. Eide, Identification of a family of zinc transporter genes from Arabidopsis that respond to zinc deficiency, *Proc. Natl. Acad. Sci. U. S. A.*, 1998, **95**, 7220–7224.

55 A. T. McKie, P. Marciani, A. Rolfs, K. Brennan, K. Wehr, D. Barrow, S. Miret, A. Bomford, T. J. Peters, F. Farzaneh, M. A. Hediger, M. W. Hentze and R. J. Simpson, A novel duodenal iron-regulated transporter, IREG1, implicated in the basolateral transfer of iron to the circulation, *Mol. Cell*, 2000, **5**, 299–309.

56 A. T. McKie, D. Barrow, G. O. Latunde-Dada, A. Rolfs, G. Sager, E. Mudaly, M. Mudaly, C. Richardson, D. Barlow, A. Bomford, T. J. Peters, K. B. Raja, S. Shirali,

M. A. Hediger, F. Farzaneh and R. J. Simpson, An iron-regulated ferric reductase associated with the absorption of dietary iron, *Science*, 2001, **291**, 1755–1759.

57 N. Z. Baquer, J. S. Hothersall, A. L. Greenbaum and P. McLean, The modifying effect of manganese on the enzymic profiles and pathways of carbohydrate metabolism in rat liver and adipose tissue during development, *Biochem. Biophys. Res. Commun.*, 1975, **62**, 634–641.

58 D. L. Baly, D. L. Curry, C. L. Keen and L. S. Hurley, Effect of manganese deficiency on insulin secretion and carbohydrate homeostasis in rats, *J. Nutr.*, 1984, **114**, 1438–1446.

59 G. Frost, C. W. Asling and M. M. Nelson, Skeletal deformities in manganese-deficient rats, *Anat. Rec.*, 1959, **134**, 37–53.

60 L. S. Hurley, E. Wooten, G. J. Everson and C. W. Asling, Anomalous development of ossification in the inner ear of offspring of manganese-deficient rats, *J. Nutr.*, 1960, **71**, 15–19.

61 A. C. Liu, B. S. Heinrichs and R. M. Leach Jr., Influence of manganese deficiency on the characteristics of proteoglycans of avian epiphyseal growth plate cartilage, *Poult. Sci.*, 1994, **73**, 663–669.

62 R. M. Hill, D. E. Holtkamp, A. R. Buchanan and E. K. Rutledge, Manganese deficiency in rats with relation to ataxia and loss of equilibrium, *J. Nutr.*, 1950, **41**, 359–371.

63 L. S. Hurley, G. J. Everson and J. F. Geiger, Manganese deficiency in rats: congenital nature of ataxia, *J. Nutr.*, 1958, **66**, 309–319.

64 B. Roussel and B. Renaud, Effect of chronic manganese intoxication on the sleep-wake cycle in the rat, *Neurosci. Lett.*, 1977, **4**, 55–60.

65 K. Mandilaras, T. Pathmanathan and F. Missirlis, Iron absorption in Drosophila melanogaster, *Nutrients*, 2013, **5**, 1622–1647.

66 X. Tang and B. Zhou, Iron homeostasis in insects: Insights from Drosophila studies, *IUBMB Life*, 2013, **65**, 863–872.

67 A. Southon, R. Burke and J. Camakaris, What can flies tell us about copper homeostasis?, *Metallomics*, 2013, **5**, 1346–1356.

68 J. A. Navarro and S. Schneuwly, Copper and Zinc Homeostasis: Lessons from Drosophila melanogaster, *Front. Genet.*, 2017, **8**, 223.

69 G. Xiao and B. Zhou, What can flies tell us about zinc homeostasis?, *Arch. Biochem. Biophys.*, 2016, **611**, 134–141.

70 C. D. Richards and R. Burke, A fly's eye view of zinc homeostasis: Novel insights into the genetic control of zinc metabolism from Drosophila, *Arch. Biochem. Biophys.*, 2016, **611**, 142–149.

71 S. E. Mohr, K. Rudd, Y. Hu, W. R. Song, Q. Gilly, M. Buckner, B. E. Housden, C. Kelley, J. Zirin, R. Tao, G. Amador, K. Sierzputowska, A. Comjean and N. Perrimon, Zinc Detoxification: A Functional Genomics and Transcriptomics Analysis in Drosophila melanogaster Cultured Cells, *G3*, 2018, **8**, 631–641.

72 M. W. Jones, M. D. de Jonge, S. A. James and R. Burke, Elemental mapping of the entire intact Drosophila gastrointestinal tract, *JBIC, J. Biol. Inorg. Chem.*, 2015, **20**, 979–987.

73 A. Rosas-Arellano, J. Vasquez-Procopio, A. Gambis, L. M. Blowes, H. Steller, B. Mollereau and F. Missirlis, Ferritin Assembly in Enterocytes of Drosophila melanogaster, *Int. J. Mol. Sci.*, 2016, **17**, 27.

74 J. A. Dow, The essential roles of metal ions in insect homeostasis and physiology, *Curr. Opin. Insect. Sci.*, 2017, **23**, 43–50.

75 C. Tejeda-Guzman, A. Rosas-Arellano, T. Kroll, S. M. Webb, M. Barajas-Aceves, B. Osorio and F. Missirlis, Biogenesis of zinc storage granules in Drosophila melanogaster, *J. Exp. Biol.*, 2018, 221.

76 I. Miguel-Aliaga, H. Jasper and B. Lemaitre, Anatomy and Physiology of the Digestive Tract of Drosophila melanogaster, *Genetics*, 2018, **210**, 357–396.

77 G. Xiao, Z. H. Liu, M. Zhao, H. L. Wang and B. Zhou, Transferrin 1 Functions in Iron Trafficking and Genetically Interacts with Ferritin in Drosophila melanogaster, *Cell Rep.*, 2019, **26**, 748–758.e745.

78 K. Balamurugan, D. Egli, H. Hua, R. Rajaram, G. Seisenbacher, O. Georgiev and W. Schaffner, Copper homeostasis in Drosophila by complex interplay of import, storage and behavioral avoidance, *EMBO J.*, 2007, **26**, 1035–1044.

79 K. Mandilaras and F. Missirlis, Genes for iron metabolism influence circadian rhythms in Drosophila melanogaster, *Metallomics*, 2012, **4**, 928–936.

80 N. Gonzalez-Morales, M. A. Mendoza-Ortiz, L. M. Blowes, F. Missirlis and J. R. Riesgo-Escovar, Ferritin Is Required in Multiple Tissues during Drosophila melanogaster Development, *PLoS One*, 2015, **10**, e0133499.

81 J. V. Llorens, C. Metzendorf, F. Missirlis and M. I. Lind, Mitochondrial iron supply is required for the developmental pulse of ecdysone biosynthesis that initiates metamorphosis in Drosophila melanogaster, *JBIC, J. Biol. Inorg. Chem.*, 2015, **20**, 1229–1238.

82 C. D. Richards, C. G. Warr and R. Burke, A role for the Drosophila zinc transporter Zip88E in protecting against dietary zinc toxicity, *PLoS One*, 2017, **12**, e0181237.

83 A. C. Jacomin, K. Geraki, J. Brooks, V. Tjendana-Tjhin, J. F. Collingwood and I. P. Nezis, Impact of Autophagy and Aging on Iron Load and Ferritin in Drosophila Brain, *Front. Cell Dev. Biol.*, 2019, **7**, 142.

84 N. Huynh, Q. Ou, L. Cox, R. Lill and K. King-Jones, Glycogen branching enzyme controls cellular iron homeostasis via Iron Regulatory Protein 1 and mitoNEET, *Nat. Commun.*, 2019, **10**, 5463.

85 P. Calap-Quintana, J. Gonzalez-Fernandez, N. Sebastia-Ortega, J. V. Llorens and M. D. Molto, Drosophila melanogaster Models of Metal-Related Human Diseases and Metal Toxicity, *Int. J. Mol. Sci.*, 2017, **18**, E1456.

86 V. Monnier, J. V. Llorens and J. A. Navarro, Impact of Drosophila Models in the Study and Treatment of Friedreich's Ataxia, *Int. J. Mol. Sci.*, 2018, **19**, E1989.

87 G. Xiao and B. Zhou, ZIP13: A Study of Drosophila Offers an Alternative Explanation for the Corresponding Human Disease, *Front. Genet.*, 2017, **8**, 234.

88 L. Gutierrez, K. Zubow, J. Nield, A. Gambis, B. Mollereau, F. J. Lazaro and F. Missirlis, Biophysical and genetic analysis of iron partitioning and ferritin function in Drosophila melanogaster, *Metallomics*, 2013, **5**, 997–1005.

89 J. E. Hwang, M. de Bruyne, C. G. Warr and R. Burke, Copper overload and deficiency both adversely affect the central nervous system of Drosophila, *Metallomics*, 2014, **6**, 2223–2229.

90 L. Gutierrez, N. Sabaratnam, R. Aktar, L. Bettedi, K. Mandilaras and F. Missirlis, Zinc accumulation in heterozygous mutants of fumble, the pantothenate kinase homologue of Drosophila, *FEBS Lett.*, 2010, **584**, 2942–2946.

91 J. H. Sang, The quantitative nutritional requirements of Drosophila melanogaster, *J. Exp. Biol.*, 1956, **33**, 45–72.

92 S. A. Blatch and J. F. Harrison, An Updated Chemically-Defined Medium for Drosophila melanogaster, *Drosoph. Inf. Serv.*, 2005, **88**, 126–128.

93 P. Rempoulakis, N. Afshar, B. Osorio, M. Barajas-Aceves, J. Szular, S. Ahmad, T. Dammalage, U. S. Tomas, E. Nemny-Lavy, M. Salomon, M. J. Vreysen, D. Nestel and F. Missirlis, Conserved metallomics in two insect families evolving separately for a hundred million years, *Biometals*, 2014, **27**, 1323–1335.

94 W. C. Lee and C. A. Micchelli, Development and characterization of a chemically defined food for Drosophila, *PLoS One*, 2013, **8**, e67308.

95 M. D. Piper, E. Blanc, R. Leitao-Goncalves, M. Yang, X. He, N. J. Linford, M. P. Hoddinott, C. Hopfen, G. A. Soultoukis, C. Niemeyer, F. Kerr, S. D. Pletcher, C. Ribeiro and L. Partridge, A holidic medium for Drosophila melanogaster, *Nat. Methods*, 2014, **11**, 100–105.

96 T. Reis, Effects of Synthetic Diets Enriched in Specific Nutrients on Drosophila Development, Body Fat, and Lifespan, *PLoS One*, 2016, **11**, e0146758.

97 A. M. Troen, E. E. French, J. F. Roberts, J. Selhub, J. M. Ordovas, L. D. Parnell and C. Q. Lai, Lifespan modification by glucose and methionine in Drosophila melanogaster fed a chemically defined diet, *Age*, 2007, **29**, 29–39.

98 F. Missirlis, S. Rahlfs, N. Dimopoulos, H. Bauer, K. Becker, A. Hilliker, J. P. Phillips and H. Jackle, A putative glutathione peroxidase of Drosophila encodes a thioredoxin peroxidase that provides resistance against oxidative stress but fails to complement a lack of catalase activity, *Biol. Chem.*, 2003, **384**, 463–472.

99 S. Ghosh, Tribute to Suzanne Eaton, from her lab members, *Nature*, 2019, **572**, 178.

100 V. Greco and S. Ghosh, Suzanne Eaton: 1959-2019, *Nat. Cell Biol.*, 2019, **21**, 1053–1054.

101 F. Julicher, Suzanne Eaton (1959-2019), *Development*, 2019, 146.

102 E. Knust and K. Simons, Suzanne Eaton (1959-2019): A pioneer in quantitative tissue morphogenesis, *J. Cell Biol.*, 2019, **218**, 2819–2821.

103 M. Brankatschk, S. Dunst, L. Nemetschke and S. Eaton, Delivery of circulating lipoproteins to specific neurons in the Drosophila brain regulates systemic insulin signaling, *eLife*, 2014, **3**, e02862.

104 J. B. Vincourt, F. Lionneton, G. Kratassiouk, F. Guillemin, P. Netter, D. Mainard and J. Magdalou, Establishment of a reliable method for direct proteome characterization of human articular cartilage, *Mol. Cell. Proteomics*, 2006, **5**, 1984–1995.

105 F. E. Cazares-Raga, B. Chavez-Munguia, C. Gonzalez-Calixto, A. P. Ochoa-Franco, M. A. Gawinowicz, M. H. Rodriguez and F. C. Hernandez-Hernandez, Morphological and proteomic characterization of midgut of the malaria vector Anopheles albimanus at early time after a blood feeding, *J. Proteomics*, 2014, **111**, 100–112.

106 A. Shevchenko, H. Tomas, J. Havlis, J. V. Olsen and M. Mann, In-gel digestion for mass spectrometric characterization of proteins and proteomes, *Nat. Protoc.*, 2006, **1**, 2856–2860.

107 Y. Perez-Riverol, A. Csordas, J. Bai, M. Bernal-Llinares, S. Hewapathirana, D. J. Kundu, A. Inuganti, J. Griss, G. Mayer, M. Eisenacher, E. Perez, J. Uszkoreit, J. Pfeuffer, T. Sachsenberg, S. Yilmaz, S. Tiwary, J. Cox, E. Audain, M. Walzer, A. F. Jarnuczak, T. Ternent, A. Brazma and J. A. Vizcaino, The PRIDE database and related tools and resources in 2019: improving support for quantification data, *Nucleic Acids Res.*, 2019, **47**, D442–D450.

108 G. Z. Li, J. P. Vissers, J. C. Silva, D. Golick, M. V. Gorenstein and S. J. Geromanos, Database searching and accounting of multiplexed precursor and product ion spectra from the data independent analysis of simple and complex peptide mixtures, *Proteomics*, 2009, **9**, 1696–1719.

109 S. J. Geromanos, C. Hughes, D. Golick, S. Ciavarini, M. V. Gorenstein, K. Richardson, J. B. Hoyes, J. P. Vissers and J. I. Langridge, Simulating and validating proteomics data and search results, *Proteomics*, 2011, **11**, 1189–1211.

110 S. J. Valentine, M. A. Ewing, J. M. Dilger, M. S. Glover, S. Geromanos, C. Hughes and D. E. Clemmer, Using ion mobility data to improve peptide identification: intrinsic amino acid size parameters, *J. Proteome Res.*, 2011, **10**, 2318–2329.

111 G. H. Souza, P. C. Guest and D. Martins-de-Souza, LC-MS(E), Multiplex MS/MS, Ion Mobility, and Label-Free Quantitation in Clinical Proteomics, *Methods Mol. Biol.*, 2017, **1546**, 57–73.

112 Y. Hu, R. Sopko, M. Foos, C. Kelley, I. Flockhart, N. Ammeux, X. Wang, L. Perkins, N. Perrimon and S. E. Mohr, FlyPrimerBank: an online database for Drosophila melanogaster gene expression analysis and knockdown evaluation of RNAi reagents, *G3*, 2013, **3**, 1607–1616.

113 K. J. Livak and T. D. Schmittgen, Analysis of relative gene expression data using real-time quantitative PCR and the 2(-Delta Delta C(T)) Method, *Methods*, 2001, **25**, 402–408.

114 X. Wang, Y. Wu and B. Zhou, Dietary zinc absorption is mediated by ZnT1 in Drosophila melanogaster, *FEBS J.*, 2009, **23**, 2650–2661.

115 J. C. Lye, C. D. Richards, K. Dechen, D. Paterson, M. D. de Jonge, D. L. Howard, C. G. Warr and R. Burke, Systematic

functional characterization of putative zinc transport genes and identification of zinc toxicosis phenotypes in Drosophila melanogaster, *J. Exp. Biol.*, 2012, **215**, 3254–3265.

116 G. Overend, Y. Luo, L. Henderson, A. E. Douglas, S. A. Davies and J. A. Dow, Molecular mechanism and functional significance of acid generation in the Drosophila midgut, *Sci. Rep.*, 2016, **6**, 27242.

117 K. Kirby, J. Hu, A. J. Hilliker and J. P. Phillips, RNA interference-mediated silencing of Sod2 in Drosophila leads to early adult-onset mortality and elevated endogenous oxidative stress, *Proc. Natl. Acad. Sci. U. S. A.*, 2002, **99**, 16162–16167.

118 F. Missirlis, J. Hu, K. Kirby, A. J. Hilliker, T. A. Rouault and J. P. Phillips, Compartment-specific protection of iron-sulfur proteins by superoxide dismutase, *J. Biol. Chem.*, 2003, **278**, 47365–47369.

119 F. Missirlis, J. P. Phillips and H. Jackle, Cooperative action of antioxidant defense systems in Drosophila, *Curr. Biol.*, 2001, **11**, 1272–1277.

120 A. J. Hilliker, B. Duyf, D. Evans and J. P. Phillips, Urate-null rosy mutants of Drosophila melanogaster are hypersensitive to oxygen stress, *Proc. Natl. Acad. Sci. U. S. A.*, 1992, **89**, 4343–4347.

121 S. Wicks, N. Bain, A. Duttaroy, A. J. Hilliker and J. P. Phillips, Hypoxia rescues early mortality conferred by superoxide dismutase deficiency, *Free Radical Biol. Med.*, 2009, **46**, 176–181.

122 L. S. Tain, R. Sehlke, C. Jain, M. Chokkalingam, N. Nagaraj, P. Essers, M. Rassner, S. Gronke, J. Froelich, C. Dieterich, M. Mann, N. Alic, A. Beyer and L. Partridge, A proteomic atlas of insulin signalling reveals tissue-specific mechanisms of longevity assurance, *Mol. Syst. Biol.*, 2017, **13**, 939.

123 N. Buchon, D. Osman, F. P. David, H. Y. Fang, J. P. Boquete, B. Deplancke and B. Lemaitre, Morphological and molecular characterization of adult midgut compartmentalization in Drosophila, *Cell Rep.*, 2013, **3**, 1725–1738.

124 A. Marianes and A. C. Spradling, Physiological and stem cell compartmentalization within the Drosophila midgut, *eLife*, 2013, **2**, e00886.

125 R. J. Hung, Y. Hu, R. Kirchner, F. Li, C. Xu, A. Comjean, S. G. Tattikota, W. R. Song, S. H. Sui and N. Perrimon, A cell atlas of the adult Drosophila midgut, *bioRxiv*, 2018, 410423, DOI: 10.1101/410423.

126 B. Hudry, E. de Goeij, A. Mineo, P. Gaspar, D. Hadjieconomou, C. Studd, J. B. Mokochinski, H. B. Kramer, P. Y. Placais, T. Preat and I. Miguel-Aliaga, Sex Differences in Intestinal Carbohydrate Metabolism Promote Food Intake and Sperm Maturation, *Cell*, 2019, **178**, 901–918.e916.

127 A. Bodzeta, M. Kahms and J. Klingauf, The Presynaptic v-ATPase Reversibly Disassembles and Thereby Modulates Exocytosis but Is Not Part of the Fusion Machinery, *Cell Rep.*, 2017, **20**, 1348–1359.

128 J. Wang, T. Binks, C. G. Warr and R. Burke, Vacuolar-type H(+)-ATPase subunits and the neurogenic protein big brain are required for optimal copper and zinc uptake, *Metallomics*, 2014, **6**, 2100–2108.

129 B. R. Graveley, A. N. Brooks, J. W. Carlson, M. O. Duff, J. M. Landolin, L. Yang, C. G. Artieri, M. J. van Baren, N. Boley, B. W. Booth, J. B. Brown, L. Cherbas, C. A. Davis, A. Dobin, R. Li, W. Lin, J. H. Malone, N. R. Mattiuzzo, D. Miller, D. Sturgill, B. B. Tuch, C. Zaleski, D. Zhang, M. Blanchette, S. Dudoit, B. Eads, R. E. Green, A. Hammonds, L. Jiang, P. Kapranov, L. Langton, N. Perrimon, J. E. Sandler, K. H. Wan, A. Willingham, Y. Zhang, Y. Zou, J. Andrews, P. J. Bickel, S. E. Brenner, M. R. Brent, P. Cherbas, T. R. Gingeras, R. A. Hoskins, T. C. Kaufman, B. Oliver and S. E. Celniker, The developmental transcriptome of Drosophila melanogaster, *Nature*, 2011, **471**, 473–479.

130 A. Nakanishi, J. I. Kishikawa, M. Tamakoshi, K. Mitsuoka and K. Yokoyama, Cryo EM structure of intact rotary H(+)-ATPase/synthase from Thermus thermophilus, *Nat. Commun.*, 2018, **9**, 89.

131 J. Zhao, S. Benlekbir and J. L. Rubinstein, Electron cryomicroscopy observation of rotational states in a eukaryotic V-ATPase, *Nature*, 2015, **521**, 241–245.

132 A. H. Brand and N. Perrimon, Targeted gene expression as a means of altering cell fates and generating dominant phenotypes, *Development*, 1993, **118**, 401–415.

133 M. D. Piper, Using artificial diets to understand the nutritional physiology of Drosophila melanogaster, *Curr. Opin. Insect. Sci.*, 2017, **23**, 104–111.

134 J. Mattila, E. Havula, E. Suominen, M. Teesalu, I. Surakka, R. Hynynen, H. Kilpinen, J. Vaananen, I. Hovatta, R. Kakela, S. Ripatti, T. Sandmann and V. Hietakangas, Mondo-Mlx Mediates Organismal Sugar Sensing through the Gli-Similar Transcription Factor Sugarbabe, *Cell Rep.*, 2015, **13**, 350–364.

135 I. Zinke, C. S. Schutz, J. D. Katzenberger, M. Bauer and M. J. Pankratz, Nutrient control of gene expression in Drosophila: microarray analysis of starvation and sugar-dependent response, *EMBO J.*, 2002, **21**, 6162–6173.

136 E. S. Brooks, C. L. Greer, R. Romero-Calderon, C. N. Serway, A. Grygoruk, J. M. Haimovitz, B. T. Nguyen, R. Najibi, C. J. Tabone, J. S. de Belle and D. E. Krantz, A putative vesicular transporter expressed in Drosophila mushroom bodies that mediates sexual behavior may define a neurotransmitter system, *Neuron*, 2011, **72**, 316–329.

137 B. Z. Tang, E. Meng, H. J. Zhang, X. M. Zhang, S. Asgari, Y. P. Lin, Y. Y. Lin, Z. Q. Peng, T. Qiao, X. F. Zhang and Y. M. Hou, Combination of label-free quantitative proteomics and transcriptomics reveals intraspecific venom variation between the two strains of Tetrastichus brontispae, a parasitoid of two invasive beetles, *J. Proteomics*, 2019, **192**, 37–53.

138 W. R. Blevins, T. Tavella, S. G. Moro, B. Blasco-Moreno, A. Closa-Mosquera, J. Diez, L. B. Carey and M. M. Alba, Extensive post-transcriptional buffering of gene expression in the response to severe oxidative stress in baker's yeast, *Sci. Rep.*, 2019, **9**, 11005.

139 M. L. Samson, Drosophila arginase is produced from a nonvital gene that contains the elav locus within its third intron, *J. Biol. Chem.*, 2000, **275**, 31107–31114.

140 L. R. Munneke and G. E. Collier, Cytoplasmic and mitochondrial arginine kinases in Drosophila: evidence for a single gene, *Biochem. Genet.*, 1988, **26**, 131–141.
141 T. Wallimann and H. M. Eppenberger, Properties of arginine kinase from Drosophila melanogaster, *Eur. J. Biochem.*, 1973, **38**, 180–184.
142 E. Morales-Rios, M. G. Montgomery, A. G. Leslie and J. E. Walker, Structure of ATP synthase from Paracoccus denitrificans determined by X-ray crystallography at 4.0 A resolution, *Proc. Natl. Acad. Sci. U. S. A.*, 2015, **112**, 13231–13236.
143 G. Esposito, M. Vos, S. Vilain, J. Swerts, J. De Sousa Valadas, S. Van Meensel, O. Schaap and P. Verstreken, Aconitase causes iron toxicity in Drosophila pink1 mutants, *PLoS Genet.*, 2013, **9**, e1003478.
144 I. Ferecatu, S. Goncalves, M. P. Golinelli-Cohen, M. Clemancey, A. Martelli, S. Riquier, E. Guittet, J. M. Latour, H. Puccio, J. C. Drapier, E. Lescop and C. Bouton, The diabetes drug target MitoNEET governs a novel trafficking pathway to rebuild an Fe-S cluster into cytosolic aconitase/iron regulatory protein 1, *J. Biol. Chem.*, 2014, **289**, 28070–28086.
145 I. Nemcovicova, S. Sestak, D. Rendic, M. Plskova, J. Mucha and I. B. Wilson, Characterisation of class I and II alpha-mannosidases from Drosophila melanogaster, *Glycoconjugate J.*, 2013, **30**, 899–909.
146 J. Cao, Y. Li, W. Xia, K. Reddig, W. Hu, W. Xie, H. S. Li and J. Han, A Drosophila metallophosphoesterase mediates deglycosylation of rhodopsin, *EMBO J.*, 2011, **30**, 3701–3713.
147 J. L. Folwell, C. H. Barton and D. Shepherd, Immunolocalisation of the D. melanogaster Nramp homologue Malvolio to gut and Malpighian tubules provides evidence that Malvolio and Nramp2 are orthologous, *J. Exp. Biol.*, 2006, **209**, 1988–1995.
148 V. Rodrigues, P. Y. Cheah, K. Ray and W. Chia, malvolio, the Drosophila homologue of mouse NRAMP-1 (Bcg), is expressed in macrophages and in the nervous system and is required for normal taste behaviour, *EMBO J.*, 1995, **14**, 3007–3020.
149 Y. Ben-Shahar, N. L. Dudek and G. E. Robinson, Phenotypic deconstruction reveals involvement of manganese transporter malvolio in honey bee division of labor, *J. Exp. Biol.*, 2004, **207**, 3281–3288.
150 E. Sovik, A. LaMora, G. Seehra, A. B. Barron, J. G. Duncan and Y. Ben-Shahar, Drosophila divalent metal ion transporter Malvolio is required in dopaminergic neurons for feeding decisions, *Genes, Brain Behav.*, 2017, **16**, 506–514.
151 I. A. Ehrnstorfer, E. R. Geertsma, E. Pardon, J. Steyaert and R. Dutzler, Crystal structure of a SLC11 (NRAMP) transporter reveals the basis for transition-metal ion transport, *Nat. Struct. Mol. Biol.*, 2014, **21**, 990–996.
152 B. Mackenzie and M. A. Hediger, SLC11 family of H + -coupled metal-ion transporters NRAMP1 and DMT1, *Pflugers Arch.*, 2004, **447**, 571–579.
153 A. Southon, A. Farlow, M. Norgate, R. Burke and J. Camakaris, Malvolio is a copper transporter in Drosophila melanogaster, *J. Exp. Biol.*, 2008, **211**, 709–716.
154 L. M. Garrick, K. G. Dolan, M. A. Romano and M. D. Garrick, Non-transferrin-bound iron uptake in Belgrade and normal rat erythroid cells, *J. Cell. Physiol.*, 1999, **178**, 349–358.
155 T. Yanagiya, N. Imura, S. Enomoto, Y. Kondo and S. Himeno, Suppression of a high-affinity transport system for manganese in cadmium-resistant metallothionein-null cells, *J. Pharmacol. Exp. Ther.*, 2000, **292**, 1080–1086.
156 S. Himeno, T. Yanagiya, S. Enomoto, Y. Kondo and N. Imura, Cellular cadmium uptake mediated by the transport system for manganese, *Tohoku J. Exp. Med.*, 2002, **196**, 43–50.
157 L. He, K. Girijashanker, T. P. Dalton, J. Reed, H. Li, M. Soleimani and D. W. Nebert, ZIP8, member of the solute-carrier-39 (SLC39) metal-transporter family: characterization of transporter properties, *Mol. Pharmacol.*, 2006, **70**, 171–180.
158 H. Fujishiro, Y. Yano, Y. Takada, M. Tanihara and S. Himeno, Roles of ZIP8, ZIP14, and DMT1 in transport of cadmium and manganese in mouse kidney proximal tubule cells, *Metallomics*, 2012, **4**, 700–708.
159 I. F. Scheiber, Y. Wu, S. E. Morgan and N. Zhao, The intestinal metal transporter ZIP14 maintains systemic manganese homeostasis, *J. Biol. Chem.*, 2019, **294**, 9147–9160.
160 M. Levy, N. Elkoshi, S. Barber-Zucker, E. Hoch, R. Zarivach, M. Hershfinkel and I. Sekler, Zinc transporter 10 (ZnT10)-dependent extrusion of cellular Mn(2 +) is driven by an active Ca(2 +)-coupled exchange, *J. Biol. Chem.*, 2019, **294**, 5879–5889.
161 D. Leyva-Illades, P. Chen, C. E. Zogzas, S. Hutchens, J. M. Mercado, C. D. Swaim, R. A. Morrisett, A. B. Bowman, M. Aschner and S. Mukhopadhyay, SLC30A10 is a cell surface-localized manganese efflux transporter, and parkinsonism-causing mutations block its intracellular trafficking and efflux activity, *J. Neurosci.*, 2014, **34**, 14079–14095.
162 Y. Nishito, N. Tsuji, H. Fujishiro, T. A. Takeda, T. Yamazaki, F. Teranishi, F. Okazaki, A. Matsunaga, K. Tuschl, R. Rao, S. Kono, H. Miyajima, H. Narita, S. Himeno and T. Kambe, Direct Comparison of Manganese Detoxification/Efflux Proteins and Molecular Characterization of ZnT10 Protein as a Manganese Transporter, *J. Biol. Chem.*, 2016, **291**, 14773–14787.
163 C. A. Taylor, S. Hutchens, C. Liu, T. Jursa, W. Shawlot, M. Aschner, D. R. Smith and S. Mukhopadhyay, SLC30A10 transporter in the digestive system regulates brain manganese under basal conditions while brain SLC30A10 protects against neurotoxicity, *J. Biol. Chem.*, 2019, **294**, 1860–1876.
164 G. Storelli, H. J. Nam, J. Simcox, C. J. Villanueva and C. S. Thummel, Drosophila HNF4 Directs a Switch in Lipid Metabolism that Supports the Transition to Adulthood, *Dev. Cell*, 2019, **48**, 200–214.e206.
165 N. D. Bond, A. Nelliot, M. K. Bernardo, M. A. Ayerh, K. A. Gorski, D. K. Hoshizaki and C. T. Woodard, ssFTZ-F1 and

Matrix metalloproteinase 2 are required for fat-body remodeling in Drosophila, *Dev. Biol.*, 2011, **360**, 286–296.

166 Q. Jia, S. Liu, D. Wen, Y. Cheng, W. G. Bendena, J. Wang and S. Li, Juvenile hormone and 20-hydroxyecdysone coordinately control the developmental timing of matrix metalloproteinase-induced fat body cell dissociation, *J. Biol. Chem.*, 2017, **292**, 21504–21516.

167 A. Balling, G. M. Technau and M. Heisenberg, Are the structural changes in adult Drosophila mushroom bodies memory traces? Studies on biochemical learning mutants, *J. Neurogenet.*, 2007, **21**, 209–217.

168 K. Kato, T. Awasaki and K. Ito, Neuronal programmed cell death induces glial cell division in the adult Drosophila brain, *Development*, 2009, **136**, 51–59.

169 H. Hall, J. Ma, S. Shekhar, W. D. Leon-Salas and V. M. Weake, Blue light induces a neuroprotective gene expression program in Drosophila photoreceptors, *BMC Neurosci.*, 2018, **19**, 43.

170 K. J. Argue, A. J. Yun and W. S. Neckameyer, Early manipulation of juvenile hormone has sexually dimorphic effects on mature adult behavior in Drosophila melanogaster, *Horm. Behav.*, 2013, **64**, 589–597.

171 M. Koppik, J. H. Specker, I. Lindenbaum and C. Fricke, Physiological Maturation Lags Behind Behavioral Maturation in Newly Eclosed Drosophila melanogaster Males, *Yale J. Biol. Med.*, 2018, **91**, 399–408.

172 X. Li, H. Ishimoto and A. Kamikouchi, Auditory experience controls the maturation of song discrimination and sexual response in Drosophila, *eLife*, 2018, **7**, e34348.

173 M. Sadraie and F. Missirlis, Evidence for evolutionary constraints in Drosophila metal biology, *Biometals*, 2011, **24**, 679–686.

174 D. P. Leader, S. A. Krause, A. Pandit, S. A. Davies and J. A. T. Dow, FlyAtlas 2: a new version of the Drosophila melanogaster expression atlas with RNA-Seq, miRNA-Seq and sex-specific data, *Nucleic Acids Res.*, 2018, **46**, D809–D815.

175 S. W. Robinson, P. Herzyk, J. A. Dow and D. P. Leader, FlyAtlas: database of gene expression in the tissues of Drosophila melanogaster, *Nucleic Acids Res.*, 2013, **41**, D744–750.

176 M. I. Lind, F. Missirlis, O. Melefors, H. Uhrigshardt, K. Kirby, J. P. Phillips, K. Soderhall and T. A. Rouault, Of two cytosolic aconitases expressed in Drosophila, only one functions as an iron-regulatory protein, *J. Biol. Chem.*, 2006, **281**, 18707–18714.

177 F. Missirlis, S. Kosmidis, T. Brody, M. Mavrakis, S. Holmberg, W. F. Odenwald, E. M. Skoulakis and T. A. Rouault, Homeostatic mechanisms for iron storage revealed by genetic manipulations and live imaging of Drosophila ferritin, *Genetics*, 2007, **177**, 89–100.

178 X. Tang and B. Zhou, Ferritin is the key to dietary iron absorption and tissue iron detoxification in Drosophila melanogaster, *FEBS J.*, 2013, **27**, 288–298.

179 X. Quan, Y. Sato-Miyata, M. Tsuda, K. Muramatsu, T. Asano, S. Takeo and T. Aigaki, Deficiency of succinyl-CoA synthetase alpha subunit delays development, impairs locomotor activity and reduces survival under starvation in Drosophila, *Biochem. Biophys. Res. Commun.*, 2017, **483**, 566–571.

180 Y. Matsushima, Y. Goto and L. S. Kaguni, Mitochondrial Lon protease regulates mitochondrial DNA copy number and transcription by selective degradation of mitochondrial transcription factor A (TFAM), *Proc. Natl. Acad. Sci. U. S. A.*, 2010, **107**, 18410–18415.

181 D. R. Littler, S. J. Harrop, L. J. Brown, G. J. Pankhurst, A. V. Mynott, P. Luciani, R. A. Mandyam, M. Mazzanti, S. Tanda, M. A. Berryman, S. N. Breit and P. M. Curmi, Comparison of vertebrate and invertebrate CLIC proteins: the crystal structures of Caenorhabditis elegans EXC-4 and Drosophila melanogaster DmCLIC, *Proteins*, 2008, **71**, 364–378.

182 N. Otto, Z. Marelja, A. Schoofs, H. Kranenburg, J. Bittern, K. Yildirim, D. Berh, M. Bethke, S. Thomas, S. Rode, B. Risse, X. Jiang, M. Pankratz, S. Leimkuhler and C. Klambt, The sulfite oxidase Shopper controls neuronal activity by regulating glutamate homeostasis in Drosophila ensheathing glia, *Nat. Commun.*, 2018, **9**, 3514.

183 W. F. Chen, S. Maguire, M. Sowcik, W. Luo, K. Koh and A. Sehgal, A neuron-glia interaction involving GABA transaminase contributes to sleep loss in sleepless mutants, *Mol. Psychiatry*, 2015, **20**, 240–251.

184 M. R. Freeman, J. Delrow, J. Kim, E. Johnson and C. Q. Doe, Unwrapping glial biology: Gcm target genes regulating glial development, diversification, and function, *Neuron*, 2003, **38**, 567–580.

185 N. Sienkiewicz, H. B. Ong and A. H. Fairlamb, Characterisation of a putative glutamate 5-kinase from Leishmania donovani, *FEBS J.*, 2018, **285**, 2662–2678.

186 B. A. Chase and D. R. Kankel, A genetic analysis of glutamatergic function in Drosophila, *J. Neurobiol.*, 1987, **18**, 15–41.

187 J. A. Fraser, R. D. Saunders and L. I. McLellan, Drosophila melanogaster glutamate-cysteine ligase activity is regulated by a modifier subunit with a mechanism of action similar to that of the mammalian form, *J. Biol. Chem.*, 2002, **277**, 1158–1165.

188 P. Lunetti, A. R. Cappello, R. M. Marsano, C. L. Pierri, C. Carrisi, E. Martello, C. Caggese, V. Dolce and L. Capobianco, Mitochondrial glutamate carriers from Drosophila melanogaster: biochemical, evolutionary and modeling studies, *Biochim. Biophys. Acta*, 2013, **1827**, 1245–1255.

189 S. Hebbar, I. Sahoo, A. Matysik, I. Argudo Garcia, K. A. Osborne, C. Papan, F. Torta, P. Narayanaswamy, X. H. Fun, M. R. Wenk, A. Shevchenko, D. Schwudke and R. Kraut, Ceramides And Stress Signalling Intersect With Autophagic Defects In Neurodegenerative Drosophila blue cheese (bchs) Mutants, *Sci. Rep.*, 2015, **5**, 15926.

190 B. C. Verrelli and W. F. Eanes, The functional impact of Pgm amino acid polymorphism on glycogen content in Drosophila melanogaster, *Genetics*, 2001, **159**, 201–210.

191 C. T. Wang, Y. C. Chen, Y. Y. Wang, M. H. Huang, T. L. Yen, H. Li, C. J. Liang, T. K. Sang, S. C. Ciou, C. H. Yuh, C. Y. Wang, T. J. Brummel and H. D. Wang, Reduced neuronal expression of ribose-5-phosphate isomerase enhances tolerance to oxidative stress, extends lifespan, and attenuates polyglutamine toxicity in Drosophila, *Aging Cell*, 2012, **11**, 93–103.

192 A. L. Knight, X. Yan, S. Hamamichi, R. R. Ajjuri, J. R. Mazzulli, M. W. Zhang, J. G. Daigle, S. Zhang, A. R. Borom, L. R. Roberts, S. K. Lee, S. M. DeLeon, C. Viollet-Djelassi, D. Krainc, J. M. O'Donnell, K. A. Caldwell and G. A. Caldwell, The glycolytic enzyme, GPI, is a functionally conserved modifier of dopaminergic neurodegeneration in Parkinson's models, *Cell Metab.*, 2014, **20**, 145–157.

193 J. Ross, H. Jiang, M. R. Kanost and Y. Wang, Serine proteases and their homologs in the Drosophila melanogaster genome: an initial analysis of sequence conservation and phylogenetic relationships, *Gene*, 2003, **304**, 117–131.

194 T. M. Khlebodarova, N. E. Gruntenko, L. G. Grenback, M. Z. Sukhanova, M. M. Mazurov, I. Y. Rauschenbach, B. A. Tomas and B. D. Hammock, A comparative analysis of juvenile hormone metabolyzing enzymes in two species of Drosophila during development, *Insect Biochem. Mol. Biol.*, 1996, **26**, 829–835.

